Identification and Characterization of Archaeal Pseudomurein Biosynthesis Genes through Pangenomics

Valérian Lupo [1,2], Célyne Roomans [1], Edmée Royen [1], Loïc Ongena [1], Olivier Jacquemin [1], Coralie Mullender [1], Frédéric Kerff [2], Denis Baurain [1,#]

[1] InBioS-PhytoSYSTEMS, Eukaryotic Phylogenomics, University of Liège, Liège, Belgium
[2] InBioS, Center for Protein Engineering, University of Liège, Liège, Belgium

Address correspondence to:
Denis Baurain: denis.baurain@uliege.be

Keywords

pseudomurein, peptidoglycan, cell wall, synteny, Mur ligases, ATP-grasp, MraY-like, inter-domain HGT, phylogenetic inference

Abstract

The peptidoglycan (PG; or murein) is a mesh-like structure, which is made of glycan polymers connected by short peptides and surrounds the cell membrane of nearly all bacterial species. In contrast, there is no PG counterpart that would be universally found in Archaea, but rather various polymers that are specific to some lineages. Methanopyrales and Methanobacteriales are two orders of Euryarchaeota that harbor pseudomurein (PM), a structural analogue of the bacterial PG. Owing to the differences between PG and PM biosynthesis, some have argued that the origin of both polymers is not connected. However, recents studies have revealed that the genomes of PM-containing Archaea encode homologues of the bacterial genes involved in PG biosynthesis, even though neither their specific functions nor the relationships within the corresponding inter-domain phylogenies have been investigated so far. In this work, we devised a pangenomic bioinformatic pipeline to

identify proteins for PM biosynthesis in Archaea without prior genetic knowledge. The taxonomic distribution and evolutionary relationships of the candidate proteins were studied in detail in Archaea and Bacteria through HMM sequence mining and phylogenetic inference of the Mur domain-containing family, the ATP-grasp superfamily and the MraY-like family. Our results show that archaeal muramyl ligases are of bacterial origin, but diversified through a mixture of horizontal gene transfers and gene duplications. However, in the ATP-grasp and MraY-like families, the archaeal members were not found to originate from Bacteria. Our pangenomic approach further identified five new genes potentially involved in PM synthesis and that would deserve functional characterization.

Introduction

The cell wall is a complex structure that surrounds most prokaryotic cells, protects them against the environment and maintains their internal turgor pressure (1, 2). It also constitutes one of the striking phenotypic differences between Archaea and Bacteria. Indeed, while most archaeal species possess a paracrystalline protein surface layer (S-layer; Rodrigues-Oliveira et al. 2017), other species harbor a large variety of cell-wall polymers (e.g., sulfated heteropolysaccharides, glutaminylglycan, methanochondroitin) (2, 4), whereas nearly all bacterial cell walls contain a single common polymer termed peptidoglycan (PG; also known as murein) (1, 5). PG is a net-like polymer formed by long glycosidic chains of alternating N-acetylglucosamine (GlcNAc) and N-acetylmuramic acid (MurNAc) units linked by a β-(1→4) bond. To MurNAc is attached a short peptide, from three to five amino acids (AA) long, usually composed of L-alanine (L-Ala), D-glutamic acid (D-Glu), meso-diaminopimelic acid (meso-DAP) or L-lysine (L-Lys), and two D-alanines (D-Ala). This short peptide serves as a bridge between two glycosidic chains and is built at the final stage of PG biosynthesis (1, 5). Interestingly, there exists an archaeal cell wall polymer that shows a three-dimensional structure similar to PG, hence named pseudopeptidoglycan or pseudomurein (PM). Compared to PG, PM contains N-

acetyl-L-talosaminuronic acid (TalNAc) units linked to GlcNAc through a β-(1→3) bond, instead of MurNAc, and only has L-amino acids attached to TalNAc (2, 6, 7). Depending on the taxon, both PG and PM can show variation in their amino acids and glucidic composition (1, 2, 5, 6). In the early 1990s, a PM biosynthesis pathway was proposed (7–9) and, due to differences between PG and PM biosynthesis, it was concluded that both polymers had evolved independently (4, 10, 11). In contrast to the ubiquity of PG, PM is found only in two orders of Euryarchaeota: Methanopyrales and Methanobacteriales. In recent phylogenomic reconstructions, Methanopyrales and Methanobacteriales are both monophyletic and further form a clade with Methanococcales as an outgroup, all three orders being collectively termed class I methanogens (12, 13). Unlike Methanopyrales and Methanobacteriales, the cell wall of Methanococcales is composed of an S-layer and does not contain PM. This restricted taxonomic distribution suggests that PM has appeared in the last common ancestor of these two orders of methanogens, after their separation from the Methanococcales lineage, and thus that PM was not a feature of a more ancient archaeal ancestor. In other studies, Methanopyrales are basal to the whole clade of class I methanogens (13, 14), which would point to a loss of PM in Methanococcales. However, it has been proposed that the latter topology might be caused by a phylogenetic artifact (15, 16).

Regarding PG, it is so crucial for cell survival and growth that even bacteria once thought to lack PG, like Planctomycetes or Chlamydiae, were actually shown to synthesize a thin layer of PG, notably during septal division (17–21). Therefore, the proteins involved in PG biosynthesis have been extensively studied over the last years, in particular as potential targets for antimicrobial agents (22). Usually, many genes involved in PG biosynthesis lie in the *dcw* (division and cell-wall synthesis) gene cluster. The order of the genes within this cluster is relatively well conserved across the different bacterial lineages (23–25), even if some species lack one or more PG biosynthesis genes in their genome (26, 27). A recent reconstruction of the ancestral state of the *dcw* cluster showed that the last bacterial common ancestor (LBCA) had a complete *dcw* cluster, probably composed of 17 genes (28).

Among the proteins encoded by *dcw* cluster genes, the four muramyl ligase

enzymes (MurC, MurD, MurE, MurF), and the D-alanine--D-alanine ligase (Ddl) are critical for PG biosynthesis. The muramyl ligases add, respectively and successively, L-Ala, D-Glu, meso-DAP (or L-Lys depending on the species) and D-Ala-D-Ala to UDP-MurNAc, while Ddl binds two D-Ala to yield the D-Ala-D-Ala dipeptide (1, 29). Inhibiting one of those genes leads to lysis of the bacterial cell (30, 31). The muramyl ligases belong to the ATP-dependent Mur domain-containing family, which further includes four other enzymes: 1) MurT, which in *Staphylococcus* forms a complex with GatD to catalyze the amidation of D-Glu to D-glutamine (D-Gln) (32, 33), 2) CapB, which plays a role in the formation of the poly-γ-glutamic acid, a polymer mainly found in *Bacillus* species, notably as the main component of the capsule of *Bacillus anthracis* (34–36), 3) cyanophycin synthetase (CphA), which catalyzes the polymerisation of L-arginine (L-Arg) and L-aspartate (L-Asp) into cyanophycin, a polymer that constitutes a nitrogen reserve in Cyanobacteria (37, 38), 4) folylpolyglutamate synthase (FPGS), which is responsible for the addition of polyglutamate to folate. The FPGS enzyme is found in the three domains of life: Archaea, Bacteria and Eukarya, but not in methanogenic archaea (39–41, 41). Ddl is part of the ATP-grasp superfamily, including at least 21 groups of enzymes (42), among which the large subunit (termed CarB) of carbamoyl phosphate synthetase (CPS; Shi et al. 2018). CPS is a well-studied enzyme that has been used to root the tree of life because CarB results from an internal gene duplication that occurred before the Last Universal Common Ancestor (LUCA) (44–46).

With the advances in genome sequencing, homologues of genes involved in PG biosynthesis, including muramyl ligases, have been identified in Methanopyrales and Methanobacteriales (47–50). Consequently, it was suggested that, despite the difference between the two biosynthetic pathways, the evolution of PG and PM are evolutionarily related, probably through horizontal transfers (HGTs) of PG biosynthetic genes from Bacteria to Archaea (51–53). Hence, Subedi and co-workers used similarity searches to re-investigate the pathway proposed by Leahy et al. 2010. They further resolved the structures of two archaeal muramyl ligases, which they named pMurC and pMurE, after their supposed homology with bacterial MurC and MurE, respectively (52, 54). While these two recent studies increased the catalog of genes potentially involved in PM biosynthesis, the homology-based approach assumes that the archaeal pathway is similar to what is known in bacteria.

Consequently, the enlarged catalog may miss key genes that are not homologous to those of the bacterial pathway while including paralogous genes that are actually not involved in PM biosynthesis (and not specific to PM-containing archaea).

In the present work, we used a pangenomic approach that did not rely on prior genetic knowledge to identify candidate genes for PM biosynthesis. Then, we characterized their functional domains using various prediction software and assessed the taxonomic distribution of their homologs in both bacterial and archaeal domains. We also investigated the evolutionary origins of PM by performing phylogenetic analyses of the Mur domain-containing family, the ATP-grasp superfamily and the MraY-like family using multiple variations of the taxon sampling and different AA substitution models. Our results confirm a bacterial origin of the four main archaeal muramyl ligases, which probably traces back to two HGT events in an ancestor of Methanopyrales and Methanobacteriales, one of these transfers being followed by two rounds of gene duplication. Yet, we arrive at different conclusions than Subedi and co-workers regarding the specific homology (and naming) of pMurC and pMurE. Finally, we identified a third gene transfer responsible for the occurrence of the complex MurT and GatD into most PM-containing archaea.

Results

Collection of candidate proteins for pseudomurein biosynthesis

For the identification of candidate genes for pseudomurein (PM) biosynthesis following a pangenomic approach independent of known genes, we used the whole proteomes of ten archaeal organisms, corresponding to five PM-containing archaea (i.e., four Methanobacteriales and one Methanopyrales) and five non-PM Euryarchaeota (i.e., one Methanococcales, two representatives from different orders of Methanomicrobia, one Archaeoglobales and one Thermoplasmatales). The protein sequences of the ten archaeal assemblies were first clustered into 6,321 orthologous groups (OGs; clusters named from OG0000001 to OG0006321). A taxonomic filter allowed us to select 82 OGs specific to the PM-containing archaea, among which 26 OGs contained sequences of all five PM-containing archaea, whereas 56 OGs contained sequences of the only Methanopyrales and three

Methanobacteriales (retained to maximize the sensitivity of our search). No OG was specific to the four Methanobacteriales. The paralogue-targeting approach (see Material and Methods) allowed us to identify 20 additional OGs. In parallel, eight OGs were selected using three pseudomurein-related HMM profiles downloaded from the NCBI CDD (Conserved Domain Database) (see Material and Methods). Overall, 110 OGs were thus identified as candidates for PM biosynthesis (Fig. S1).

Genetic environment of candidate proteins

Synteny analysis revealed that 22 out of 110 OGs are encoded by genes clustered in five regions of the genomes of PM-containing archaea, which we termed clusters A to E (Fig. S2). *In silico* functional analysis indicates (Table S1; sheets 1 to 3) that proteins of clusters A and B may be involved in PM biosynthesis while proteins of clusters C, D and E are probably not. Cluster C is a bidirectional cluster, where annotated proteins belong to different pathways. Indeed, OG0001177 and OG0001178 proteins are associated with pilus assembly proteins and/or surface proteins, while OG0001176 and OG0000094 can be associated with cell shape or gene regulation (the latter is not identified in our pipeline but its gene is always located downstream of the OG0001176 gene). Cluster D is related to nucleic acid metabolism or cellular signal transduction (55), whereas cluster E code for the four proteins that compose the methyl-coenzyme M reductase, which is implied in methane formation (56). Clusters A and B correspond to the two clusters identified by (52), based on similarity searches using bacterial PG biosynthetic proteins as queries. Cluster A is composed of five genes: 1) OG0001014, which was experimentally characterized as the smallest CPS (57), 2) OG0001163, a type 4 glycosyltransferase homologue to MraY, 3) OG0001473, a Mur domain-containing protein, 4) OG0001162 and 5) OG0001472, two hypothetical proteins devoid of known domains. Regarding cluster B, it is composed of three genes: 1) OG0001150, a Mur domain-containing protein, 2) OG0001147, another uncharacterized hypothetical protein and 3) OG0001146, a MobA-like NTP transferase domain-containing protein. In addition, two genes of Mur domain-containing proteins (i.e., OG0001148 and OG0001149) can be located either in cluster A or cluster B, and even outside any cluster, depending on the PM-containing species considered. Furthermore, another PM-specific gene (OG0000796, coding for a hypothetical

protein) is located just downstream of the OG0001472 gene in the genome of *Methanopyrus sp. KOL6*, while a second one (OG0000169, coding for a Zn peptidase) is only three genes away from the OG0001146 gene in *Methanothermobacter thermautotrophicus str. Delta*. Based on the genetic environment of clusters A and B, we attempted to identify a conserved regulon for PM biosynthesis by phylogenetic footprinting (58, 59). However, unlike in Bacteria (59), such analyses were unsuccessful on our archaeal dataset (see Supplementary data).

Taking into account OG0000094, identified by its conserved localisation within cluster C, our pipeline recovered 23 syntenic genes (out of 111 OGs), of which half are likely to be involved in PM biosynthesis (Table 1). For clarity, in the following, the four Mur domain-containing proteins OG0001148, OG0001149, OG0001150 and OG0001473 will be arbitrary called Murα, Murß, Muryγ and Murδ, respectively, without considering any specific homology with bacterial MurCDEF. Most of the proteins encoded in clusters A and B have no predicted signal peptide (SP) and are either cytoplasmic or transmembrane (TM) proteins. TM segment prediction was used as a complement to SP prediction. It allowed us to distinguish between cytoplasmic and transmembrane proteins, and revealed that only OG0000796, OG0001163 and OG0001472 are TM proteins. OG0000169 and OG0001162 feature a Sec SP and are thus the only exported proteins of these gene clusters. In PM-containing archaea, the synteny of the genes coding for OG0001472 and Murδ is highly conserved. However, in *Methanothermobacter thermautotrophicus str. Delta*, both genes were annotated as pseudogenes and thus not predicted as proteins.

Taxonomic distribution of candidate proteins and their homologues

To ensure the completeness of the selected OGs, we looked for corresponding pseudogenes or mispredicted proteins in the genomes of the five PM-containing archaea (see Material and Methods). After completing the OGs, we retained only those containing protein sequences from all five PM-containing archaea, decreasing the number of OGs from 111 to 49. Interestingly, no OG from the five syntenic regions had to be discarded. Homology searches in three local databases showed

that 15 OGs are widespread (though not universal) among Bacteria and Archaea, 9 OGs have homologues only in bacteria and PM-containing archaea, while 25 OGs are exclusive to archaea, among which 15 to PM-containing archaea (Fig. 1; for details see Table S2). In clusters A and B, which likely encode proteins involved in PM biosynthesis, 5 OGs are exclusive to Methanopyrales and Methanobacteriales whereas 7 OGs share homology with bacterial proteins. We also noticed that our HMM profiles of the four muramyl ligases (i.e., Murα, Murß, Murγ and Murδ) recovered a common set of sequences, indicating that Muraßγδ are specifically related. According to this taxonomic distribution, we further investigated the origin of OG0001014 (currently annotated as CPS), the MraY-like and the four muramyl ligases Muraßγδ. The MobA-like NTP transferase (OG0001146) was not considered for phylogenetic analyses because, compared to the aforementioned proteins, no homologous protein was identified in the representative bacterial database (nor for OG0001215 and OG0000138). However, some bacterial homologues were recovered when we determined the taxonomic distribution of the 49 OGs using the (much larger) prokaryotic database.

Phylogenetic analyses

ATP-grasp superfamily

OG0001014 from the cluster A of PM-containing archaea, as well as the Ddl from the *dcw* cluster of bacteria, are member proteins of the ATP-grasp superfamily. Due to the large number of protein functions and architectures within the ATP-grasp superfamily (42), we focused our phylogenetic analyses on the ATP-grasp domain. Furthermore, we wanted to investigate whether OG0001014 is actually a CPS, as proposed by Popa et al. 2012, or closely related to Ddl (through HGT for instance). Thus, we excluded eukaryotic ATP-grasp proteins from our analyses. In the local databases, we identified 8,013 unique protein sequences containing at least one ATP-grasp domain, which are distributed across 1,387 prokaryotic organisms. ATP-grasp domains were spliced out of full-length proteins, yielding a total of 12,074 domain sequences, then sequence deduplication led to 2,344 sequences from which 149 highly divergent sequences were removed. Annotation showed that 1,788 domain sequences correspond to 17 members of the ATP-grasp superfamily, while

407 sequences have no similarity with reference ATP-grasp sequences (see Material and Methods). We also observed that PyC, PccA and AccC reference sequences annotate proteins belonging to the same monophyletic group. These three enzymes use hydrogenocarbonate as a substrate (60–62), which could explain the phylogenetic proximity of their ATP-grasp domain sequences. Accordingly, we decided to indistinctly tag the whole group with the three annotations. Similarly, PurK and PurT reference sequences mostly annotated the same set of proteins, albeit PurK uses hydrogenocarbonate as its substrate and PurT formate (63, 64).

Due to an internal gene duplication that occurred before LUCA (44–46), the seven phylogenetic trees (see Material and Methods) were rooted on CarB, the monophyly of which is supported by high statistical values. Despite a low topology conservation between the different evolutionary models and number of tree search iterations, some recurring patterns can be observed (Fig. 2 and Fig S3 to S8). RimK ATP-grasp domain sequences are always paraphyletic, due to the inclusion of GshB, GshAB and CphA, the latter two clustering into a smaller clan. The monophyly of Acetate--CoA ligases AcD (65) is maximally supported and a long branch is present at the base of the group. Except for the C40 model (Fig S5 and S6), AcD forms a clan with the Succinate--CoA ligase SucC (66). The position of the other members of the ATP-grasp superfamily is much more elusive. For example, Pur2 (67) emerges from an unannotated region of the LG4X tree (Fig. 2), whereas it forms a clan with either AcD and SucC in the four C20 and C60 trees (Fig S3-4 and S7-8) or only with SucC in the two C40 trees (Fig S5 and S6). Similarly, albeit Ddl and OG0001014 branch together in one C20 tree with a branch support of 63 (Fig S3), their respective positions within the ATP-grasp superfamily are unstable (Fig 2 and Fig S3 to S8). In conclusion, OG0001014 is clearly not a CPS since it is never close to CarB in our trees. Moreover, there is no strong phylogenetic evidence for a specific relationship between OG0001014 and Ddl, in contrast to what we had hypothesized.

MraY-like family

Homology searches revealed that the bacterial homologue of OG0001163 is the glycosyltransferase 4 (GT4) MraY. According to the NCBI CDD (68), MraY is part of the MraY-like family, which further includes WecA (69), WbpL (70, 71), and eukaryotic and archaeal GPT (72). In addition to the MraY-like OG0001163, our

pipeline has highlighted transmembrane proteins in OG0001207 (Fig. 1), for which the only bacterial homologue also has a MraY/WecA-like GT4 domain. Therefore, we decided to add the sequences of OG0001207 to the phylogenetic analysis of the MraY-like family. Although only one sequence similar to OG0001207 had been identified in the bacterial database, 62 additional bacterial OG0001207 homologues were identified in the (larger) prokaryotic database. According to the study of Lupo et al. 2021, none of the genomes coding for those protein sequences are considered as contaminated, which suggests that OG0001207 homologues genuinely exist in these bacteria. Overall, a total of 1,267 sequences from the MraY-like family were identified in our databases, corresponding to 1,071 unique sequences. Interestingly, 773 sequences among 1,267 were identified by two or more HMM profiles of the individual members of the MraY-like family. As reference sequences of WecA and WbpL annotated putative sequences from the same monophyletic group, the whole group was considered as WecA/WbpL.

Due to this non-universal taxonomic distribution and lack of an ancestral gene that could be present in the genome of LUCA, the three MraY-like family trees (see Material and Methods) were left unrooted. Phylogenetic analysis showed that each of the five members of the MraY-like family are monophyletic and all supported by high bootstrap values. Moreover, MraY formed a clan with WecA/WbpL while GPT formed a clan with OG0001163 and OG0001207, and these relationships are similar for the three evolutionary models LG4X, C20 and C40 (Fig. 3 and Figs S9 and S10). Taxonomic analysis revealed that MraY and WecA/WbpL are exclusive to bacteria, while GPT is only found in archaea. Regarding OG0001163, it is exclusive to PM-containing archaea, as would be OG0001207, ignoring the few aforementioned exceptions. Together, the clear dichotomy between bacterial and archaeal sequences and the high statistical support (≥ 90%) at the basal branch of each member of the MraY-like family suggest that LUCA already possessed at least one copy of a *mraY-like* gene.

Mur domain-containing family

Homology searches allowed us to identify 3,398 unique sequences distributed across 755 prokaryotic organisms. These sequences correspond to 12 members of

the Mur domain-containing family, which are the four bacterial MurCDEF, the four archaeal Muraßγδ, MurT, CapB, CphA and FPGS. Taxonomic distribution within each member protein group revealed that MurCDEF and CphA are specific to bacteria, Muraßγδ are specific to PM-containing archaea, while MurT, CapB and FPGS are found both in Bacteria and Archaea, albeit not universally. According to the function and ubiquity of FPGS, we assumed that a FPGS protein was already present in LUCA, and trees were rooted on the corresponding clan. The phylogenetic trees, inferred with three models from a matrix of 3,407 sequences x 550 AAs (see Material and Methods) including the 12 members of the Mur domain-containing family, showed that each member group is monophyletic and supported by high statistical values (bootstrap support around 100; Fig S11 to S13). In spite of the solid monophyly of each Mur domain-containing family member, the recovered relationships between these members (i.e., the topology of the family tree) appear to depend on the evolutionary model. We made the same observation for phylogenetic reconstructions based on a smaller matrix, restricted to the most conserved AAs over the full-length alignment (3,386 sequences x 228 AAs) (Fig. S14 to S16).

The relationships between the four bacterial muramyl ligases MurCDEF and their uncharacterized archaeal homologues Muraßγδ were also investigated through phylogenetic analyses using only one out of four potential outgroups among MurT, CapB, CphA and FPGS, again under the three models (Fig. 4a and Fig S17 to S27). In these trees, Muraα and Murß always strongly group together (bootstrap support from 86 to 100), and further form a clan with Muryγ and MurD in 11 trees out of 12 (support between 81 and 99 in ten trees). Murδ groups with MurC in eight trees, but support is uneven and generally weaker (three trees between 95 and 100 and the five others around 50). Furthermore, MuraßγD and MurδC form a clan in five trees (support between 93 and 98 in four trees), while this larger clan further includes MurT in the three trees where it is present.

To test the robustness of the recovered relationships, we implemented a jackknife approach based on random subsets of sequences representing the 12 members of the Mur domain-containing family. The replicate trees (also built under LG4X, C20 and C40 models) were either combined into consensus trees using ASTRAL (Fig 4b and Figs S30 and S31) or automatically searched for clans of interest (see Material

and Methods for details). These resampling analyses confirmed the monophyly of each member of the Mur domain-containing family with the exception of MurT. Indeed, LG4X and C40 ASTRAL trees revealed that MurT sequences can explode into two distinct clans: 1) a large one composed of bacterial and Methanobacteriales sequences, and 2) a smaller one composed of sequences of Methanopyrales and Methanobacteriales, which we termed MurT-like. In addition, ASTRAL trees also confirmed the relationships between the eight muramyl ligases observed in the single-outgroup trees, even if those were blurred by the unstable positions of MurT and MurT-like sequences. Of note, although ASTRAL trees exhibited maximal quartet support values for the relationships between Mur domain-containing family members, the actual jackknife proportions for most clans of interest were much lower (Table S3), which indicates that the precise branching order of the members of the family remains difficult to resolve.

As *murT* and *gatD* genes are clustered in an operon in the genomes of *Staphylococcus* species (32, 74)), we performed a homology search of GatD in our local databases. This survey revealed that the Methanobacteriales and bacterial species that harbor a MurT homologue also have a GatD homologue whereas no GatD homologues are found in archaeal species that only bear MurT-like. The topology of the tree built from the concatenation of MurT and GatD sequences (Fig. 5) showed that the archaeal operon is monophyletic and emerges from Terrabacteria, with *Caldisericum exile* as the closest relative (bootstrap support of 89). In addition, the Terrabacteria sequences, represented by Bacillota (previously named Firmicutes), those of Actinomycetota (Actinobacteria) and a single sequence from Chloroflexota (Chlorofexi), are grossly intermingled. These relationships also apply to all the (larger) trees including MurT and MurT-like sequences (Fig 4a, 4b, S11 to S19 and S30 to S33), where the MurT-like clan is always basal to the MurT clan.

Overall, our analyses showed that neither MurT nor CphA should be considered as an outgroup for the Mur domain-containing family. Indeed, we observe that MurT sequences form either one or two (MurT + MurT-like) clans, which emerge from the larger clan formed by the six muramyl ligases MuraßγδCD. In spite of the difficulty to determine the exact positions of MurT and MurT-like, both regular trees and

resampling analyses tend to indicate that all MurT sequences derive from the same ancestral gene as MuraßγδCD. In contrast to the other members of the Mur domain-containing family, CphA originates from the fusion of two functional domains: 1) an ATP-grasp domain at the N-terminal region (see ATP-grasp superfamily) and 2) the Mur ligase domain at the C-terminal region. This C-terminal region appears to be closely related to MurE and MurF according to our phylogenetic inferences. Regarding CapB, resampling analyses showed that it is not related to the four bacterial muramyl ligases MurCDEF or to the four archaeal muramyl ligases Muraßγδ, but more likely to FPGS (Table S3), thus indicating that it could be used as an outgroup to study the relationships between MurCDEF and Muraßγδ. However, unlike FPGS, the taxonomic distribution of CapB is more restricted, being found only in Gammaproteobacteria, Bacilli, Synergistota (Synergistetes), Halobacteria and a few Methanosarcinales, and Korarchaota, which eventually makes it less suitable to the task than FPGS.

Discussion

Improved catalog of pseudomurein biosynthetic genes

In this study, we devised a pangenomic strategy to identify all the genes potentially involved in PM biosynthesis in Archaea. In contrast to Subedi et al. (2021), who relied on similarity searches to identify candidate genes, our protocol consisted in clustering protein sequences from the whole proteomes of five PM-containing archaea and five non-PM Euryarchaeota into OGs, followed by a semi-automated analysis of the taxonomic distribution of the resulting OGs. This strategy enabled the identification of a total of 49 OGs, among which some are exclusively specific to PM-containing archaea while others contain paralogous genes that are specific to those archaea. Only a few of them could be associated with pseudomurein biosynthesis and correspond to the two syntenic regions described in Subedi et al. 2021. With respect to the latter study, two more genes were detected due to their association with either cluster A or B in some lineages: OG0000766, a polytopic transmembrane protein, and OG0000169, an extracellular protein. Both have an unknown function but are specific to PM-containing archaea. In addition to the two clusters, the similarity searches of Subedi et al. 2021 also identified eight more genes in PM-

containing archaea: *glmS*, *glmM*, *glmU*, *galE*, *murG*, *uppS*, *uppP* and a flippase. However, our own approach did not recover these genes, an expected outcome that can be explained by two reasons: 1) genes like *glmS*, *glmM*, *glmU* or *galE* are nearly ubiquitous among prokaryotes (52) and have no specific paralogs in PM-containing archaea, 2) genes, like *murG or uppS*, are missing in some genomes of the five PM-containing archaea and; therefore, their role in PM biosynthesis is questionable. Our OG0000044 includes the transglutaminase genes mentioned in Leahy et al. 2010, which are enzymes that catalyze the bond formation between L-Glu and L-Lys residues in proteins (75) but the corresponding genes are not associated with any cluster. Yet, *in silico* predictions show that these enzymes are exported toward the extracellular space. Therefore, OG0000044 is the best candidate to perform bond formation between L-Glu in position 5 of one chain to L-Lys in position 3 of another chain during PM cross-linking. In comparison to the study of Subedi et al. 2021, we have additionally identified five OGs neither associated with cluster A or B: OG0001024, OG0001140, OG0001158, OG0001194, OG0001470. These OGs do not exhibit any known function but are exclusive to PM-containing archaea (Fig. 1). Given their taxonomic distribution, they might play a role in PM biosynthesis, though further investigation is required to confirm this hypothesis.

Origin and evolution of Mur ligases

Our phylogenetic analyses of the Mur domain-containing family show that each member of the family is monophyletic. However, the relationships between those members are difficult to resolve owing to the low remaining phylogenetic signal, and because phylogenetic artifacts, such as long-branch attraction, probably affect phylogenetic reconstruction, especially in trees including all non-Mur “outgroups” (76). Indeed, compared to MurCDEF, archaeal muramyl ligases (here termed Muraßγδ) are characterized by very long branches; for example, Murδ has experienced more than one substitution per site since its probable separation from MurC. When focussing on Mur trees with only one outgroup, the topology is quite robust to the use of different evolutionary models, as it is in species resampling analyses featuring all outgroups (Table S3). In this topology, MurD forms a clan with Muraα+Murß+Muryγ, MurC a clan with Murδ, and MurE a clan with MurF, and all these relationships are also recovered in unrooted trees devoid of any outgroup (Figs S34

to S36). Therefore, they enable the exclusion of potential evolutionary scenarios, in which LUCA would have possessed either one, two, or four *mur* genes vertically inherited by both Bacteria and Archaea (Figs 6 A-C). The first scenario implies two series of three gene duplications, independently in Bacteria and Archaea. If true, this scenario would be evidenced by a bipartition between all bacterial sequences and all archaeal sequences (Fig. 6 A). The second scenario posits a duplication event in LUCA, followed by additional gene duplications in bacterial and archaeal lineages, resulting in two mirror subtrees, each bearing two archaeal and two bacterial genes (Fig. 6 B). In the third scenario, where LUCA already possessed four *mur* genes, each archaeal gene would have been associated with its bacterial counterpart (i.e., orthologue) in the tree (Fig. 6 C). Besides, two potential scenarios where archaeal genes would have been acquired by horizontal transfer from bacteria can be ruled out (Figs 6 C-D). Indeed, the topology of Fig. 6 C would also be recovered after the transfers of the four bacterial genes to archaea, whereas a scenario involving the single transfer of any form of bacterial gene to the ancestor of PM-containing archaea, followed by three duplications, would yield a tree where the four archaeal Mur ligases emerge from bacterial Mur ligases (Fig. 6 D). Finally, it is worth noting that, in an unrooted phylogeny, the last scenario of Fig. 6 D would be indistinguishable from the first one depicted in Fig. 6 A.

As previously stated, early analyses of their biosynthetic pathways have suggested that neither PG nor PM were a feature of LUCA (4, 11, 52, 53). Therefore, LUCA probably did not possess the various muramyl ligases presently involved in cell-wall biosynthesis. Furthermore, since the LBCA already possessed a complete *dcw* gene cluster (28), and given that PM is restricted to Methanopyrales and Methanobacteriales (2), we propose a scenario for Mur ligase evolution (Fig. 6 E). In this scenario, the ancestral gene of *murCDEF* was duplicated a first time in the pre-LBCA lineage to yield the ancestral genes of *murCD* and *murEF*, followed by a second round of duplications, which led to the current four bacterial muramyl ligases. Some evidence indicates that the duplication of the *murEF* ancestral gene to yield *murE* and *murF* could have occurred later than the duplication of the *murCD* ancestral gene. In fact, *murE* and *murF* genes are always in tandem in the *dcw* cluster of most bacterial species, as well as in the reconstruction of the LBCA *dcw* cluster (28), and can even be expressed as a single fusion protein MurE-MurF (77).

Moreover, in the majority of our Mur domain-containing family trees, MurE and MurF have slightly shorter branches than those of MurC and MurD. As we rule out the scenarios involving one and four HGTs for the origin of archaeal muramyl ligases (Fig. 6 C-D), those must have stemmed from either two or three HGT events. In fact, our phylogenetic analyses consistently suggest only two instances of HGT. After the diversification of the LBCA, the *murD* gene was transferred to the common ancestor of PM-containing archaea, then *murD* experienced two duplications that yielded *murα*, *murß* and *murγ* (our nomenclature). There is strong evidence that *murα* and *murß* arose from a gene duplication: the corresponding proteins group together in almost all phylogenetic reconstructions (in both rooted and unrooted trees) and, as for MurF and MurE, their genes are in tandem in the genome of most PM-containing archaea while some Methanobrevibacter and Methanothermobacter genomes (two genera of Methanobacteriales) code for a Murα-Murß fusion protein (52). As for the first, older, duplication of *murD*, leading to *murγ* and the *muraß* ancestor, it is visible in unrooted trees, where *murα*, *murß* and *murγ* form a clan. Regarding *murδ*, the phylogenetic analyses mostly suggest a *murC* affinity, and thus an independent gene transfer event from bacteria.

Compared to other members of the Mur domain-containing family, the four bacterial and the four archaeal muramyl ligases are the only enzymes featuring three homologous structural domains (N-terminal, central and C-terminal) (78). In bacterial sequences, the N-terminal domain binds to PG precursors, the central domain binds ATP, while the C-terminal binds the AA that is transferred to the nascent pentapeptide. The N-terminal domain exhibits the highest sequence and structural diversity, whereas the central domain is the most conserved (78). In addition, the accepted dichotomy of MurC/MurD versus MurE/MurF is only based on sequence similarities and 3D structures of the N-terminal domain (78, 79). Thus, the observed varying level of conservation of the different domains probably results in a phylogenetic signal that is not uniform along the sequences. This may explain the inconsistency between the study of Subedi et al. 2022 and ours, where they associate Murδ with MurE/F, based on the structure of the N-terminal domain, whereas our phylogenetic analyses of the full-length sequences rather indicate an affinity to MurC. It is noteworthy that, in the CapB and CphA outgroup trees computed with the C40 model (Figs S22 and S25), Murδ branches inside the MurE

clan, within Bacillota. Even though such an alternative relationship would fit the conclusion of Subedi et al. 2022, the analysis of the two matrices under the more sophisticated PMSF LG+C60+G4 model (Figs S28 and S29) did not yield that latter topology, and instead supported the first solution.

Although there are several clues hinting to gene transfers of muramyl ligases from bacteria to PM-containing archaea, the archaeal sequences (Muraßγδ) never branch within bacterial muramyl ligase sequences (MurCDEF) in our phylogenetic trees, and these trees do not provide indications about the direction of the transfers. However, the apparent monophyly of each bacterial member of the family could also be an artifact due to fast-evolving sequences in archaeal species. This kind of artifact has already been reported, e.g., with plastidial genes in eukaryotes, which rarely branch within (and rather sister to) Cyanobacteria (80), although the endosymbiotic origin of the plastid is widely accepted (81). Nevertheless, we detected a clear transfer from bacteria to PM-containing archaea, involving the *murT* gene. Previously, MurT had been described in *Staphylococcus* spp*, Streptococcus pneumoniae* and *Mycobacterium tuberculosis* (32, 33, 74, 82). Here, our analyses revealed that MurT is not ubiquitous in Bacteria, being only found in Bacillota, Actinomycetota, *Caldisericum exile* (Caldisericota) and *Thermobaculum terrenum* (Chloroflexota). We also identified *murT* homologues in Archaea, specifically in Methanopyrales and Methanobacteriales. Interestingly, the bacteria that harbor MurT mostly have one copy of the *murT* gene while some PM-containing archaea have two copies, which we named *murT* and *murT-like*. Hence, Methanobacteriales can possess only MurT or only MurT-like or both, whereas the few available Methanopyrales solely have one MurT-like gene. Archaeal MurT sequences clearly group with the sequence of *C. exile*, which further branches within Terrabacteria. The tree of the MurT partner, GatD, is similar, and this topology is confirmed by the concatenation of MurT and GatD sequences. This suggests that both genes were transferred together from a Terrabacteria lineage, with *C. exile* as the closest extant relative of the donor lineage. Establishing the exact phylogenetic position of *C. exile* in the bacterial diversity remains challenging due to the limited genomic data available for Caldisericota. In 2022, (28)showed that *C. exile* may lie between Terrabacteria and Gracilicutes, which means that it could be affiliated to one or the other superphylum, depending on the rooting of the bacterial tree. The taxonomic distribution MurT and

GatD among bacteria suggests that *C. exile* might belong to Terrabacteria, and thus rather be on the monoderm side in terms of cell-wall architecture. A recent study reinforces this view by positioning Caldisericota within Terrabacteria, but still based on the same single genome (83). According to the taxonomic distribution of archaeal MurT/GatD and Muraßγδ, we hypothesize that the gene transfers of *murT*/*gatD* and the two ancestor genes of *muraßγδ* both occurred before the diversification of PM-containing archaea. In contrast, the origin of the *murT-like* gene is enigmatic, owing to its position basal to the MurT clan, even though one possible explanation would be a duplication of *murT* in the last common ancestor of Methanopyrales and Methanobacteriales, followed by differential losses of either *murT*/*gatD* or *murT-like* in descendant lineages.

Uncompelling evidence for Ddl and MraY orthologues in Archaea

In cluster A, there are two adjacent genes, OG0001014 and OG0001163, that show a homology with genes of the bacterial *dcw* gene cluster, respectively *ddl* and *mraY*. Both genes are exclusive to Methanopyrales and Methanobacteriales species. Thus, it has been proposed that their products are probably involved in PM biosynthesis (52). Having concluded that archaeal muramyl genes originate from gene transfers from an ancient bacterial lineage, we further investigated whether OG0001014 and OG0001163 genes were also transferred from bacteria. However, our extensive phylogenetic analyses of the ATP-grasp superfamily and the MarY-like family revealed that neither OG0001014 nor OG0001163 are specifically associated with Dld or MraY. Indeed, although trees of the ATP-grasp domain show members of the superfamily that are mostly monophyletic and supported by high statistical values, the position of Ddl and OG0001014 in the tree is not stable across our seven trees. In addition, OG0001014 never clusters with Ddl (except in the C20 tree; support value of 63) but always features a long branch, which can explain the difficulty to position it accurately (i.e., long-branch attraction artifact). In 2012, (57) experimentally characterized OG0001014 and concluded that it was the smallest CPS closely related to the large subunit of a “true” CPS, CarB. However, OG0001014 never groups with CarB in any of our trees while its genetic environment suggests that it is involved in PM biosynthesis. For their part, Subedi et al. 2021,

proposed that OG0001014 could be involved in the three-step activation of L-Glu to UDP-N-glutamyl-γ-phosphate (UDP-N-Glu-γ-P). Based on these ideas and our own observations, we propose that the reported CPS function of this enzyme might not be correct and that the kinase activity measured by Popa et al. actually plays a role in the addition of a phosphate to L-Glu, either in the first step to form N^{α}-P-Glu or in the third step to form UDP-N^{α}-Glu-γ-P (9).

Regarding the phylogenetic analyses of the MraY-like family, the archaeal MraY-like does not appear to have evolved from the bacterial MraY. Indeed, bacterial and archaeal proteins are clearly separated in all unrooted phylogenetic trees, although archaeal monophyletic groups are characterized by long branches, especially OG0001207, which could lead to strong phylogenetic artifacts. In contrast to Mur domain-containing family and ATP-grasp superfamily trees, MraY-like family trees were left unrooted. In fact, none of the MraY-like family members is found in both Bacteria and Archaea. As shown in the Results section, MraY and WecA/WbpL are only present in bacterial species, GTP is ubiquitous in archaea while MraY-like and OG0001207 are exclusive to PM-containing archaea. In addition, WecA/WbpL is the only monophyletic group where some organisms bear two sequences, which could indicate that WecA and WbpL are two paralogues. According to the taxonomic distribution of MraY, WecA/WbpL and GPT, we propose a scenario where an ancestral GT4 gene found in LUCA was vertically transmitted to both Archaea (GPT) and Bacteria (the ancestral gene coding for both MraY and WecA/WbpL). The bacterial gene was then duplicated once to yield *mraY* and *wecA/wbpL*. Thus, GPT would be the orthologue of MraY and WecA/WbpL, while MraY and WecA/WbpL would be paralogous. For this phylogenetic analysis of the MraY-like family, we followed the family as defined in the NCBI CDD (https://www.ncbi.nlm.nih.gov/Structure/cdd/cddsrv.cgi?uid=264002) to increase the sequence sampling. In theory, it is possible that we undersampled the family. Indeed, the GT4 domain is also present in other proteins, like MurG (77, 84), which are not part of the MraY-like family. A proper way to study the origin of the MraY-like family would be to infer a phylogenetic tree of the GT4 domain (as we did for the ATP-grasp domain). However, such an analysis would be very time-consuming due to the large number of GT sequences (85). For now, overlapping HMM search results starting from the different family members do not suggest any undersampling

issue. Actually, it could be the opposite, with our tree including sequences that are not part of the MraY-like family, such as the bacterial homologues of OG0001207, which have a very long branch in spite of featuring a MraY/WecA-like GT4 domain.

Nature of the ancestral cell wall

The current architecture of PG and PM are well-known, but it is clear that both polymers were different in their early evolutionary state, i.e., before acquisition and diversification of their respective muramyl ligases. However, inferring the ancestral states of PG and PM is almost impossible because those evolved in the stem branch of Bacteria or class I methanogens Archaea (including both Methanobacteriales and Methanopyrales), respectively, before the last common ancestors of extant organisms. As other Mur-domain containing proteins, like CapB, FPGS, MurT or CphA, bind amino acids with an α-carboxylic acid group (i.e., aspartic acid and glutamic acid), we speculate that the first muramyl ligase proteins were also associated with those AAs. Moreover, glutamic acid is one of the most abundant AAs in many organisms, and it participates in a wide array of metabolisms (86). Therefore, glutamic acid could be one of the first AAs to have been selected by muramyl ligases. In *Bacillus*, the complex formed by CapB, CapC, CapA and CapE recruits L-Glu or D-Glu to synthesize the poly-γ-glutamic acid capsule. This kind of cell wall has also been suggested to occur in *Haloquadratum walsbyi*, based on genomic analyses. *H. walsbyi* is classified in Halobacteria, a class of Euryarchaeota characterized by a diverse variety of cell walls: S-layer, sulfated heteropolysaccharides, halomucin and glutaminylglycan. The latter is composed of poly-γ-L-glutamate, to which are linked two types of oligosaccharides (2). Analyses showed that CapB is ubiquitous in Halobacteria, indicating that CapB could be involved in glutaminylglycan biosynthesis. Consequently, we suggest that this simpler cell wall could resemble the ancient forms of PG and/or PM.

Material and Methods

Data availability

Publicly available datasets, including all detailed YAML configuration files used with Forty-Two (87, 88) and classify-ali.pl (D. Baurain; https://metacpan.org/dist/Bio-MUST-Core), and a detailed command line log file can be found here: https://doi.org/10.6084/m9.figshare.21641612.

Protein sequence databases

Three local mirrors of NCBI RefSeq were used during this study: 1) an archaeal database composed of the 819 whole genomes that were available on March 7, 2019, 2) a bacterial database of 598 representative genomes selected by the ToRQuEMaDA pipeline (89) and 3) a prokaryotic database of 80,490 genomes, already used in (90). To assemble the bacterial database, ToRQuEMaDA was run in June 2018, according to a 'direct' strategy and using the following parameters: dist-metric set to JI (Jaccard Index), dist-threshold set to 0.86, clustering-mode set to 'loose', and pack size set to 200.

Identification of candidate proteins for pseudomurein biosynthesis

Protein orthologous groups (OGs) were built from the conceptual translations of ten archaeal whole genomes using OrthoFinder v2.2.1 (91) with default parameters. These archaeal genomes correspond to five organisms having pseudomurein (PM) (GCF_000008645.1, GCF_000016525.1, GCF_000166095.1, GCF_002201915.1, GCF_900095295.1) and five without PM (GCF_000011185.1, GCF_000013445.1, GCF_000017165.1, GCF_000025285.1, GCF_000251105.1) and were downloaded from the NCBI RefSeq database on March 7th, 2019. Then, taxonomic filters were applied to the OGs using classify-ali.pl v0.212670 in order to select candidate proteins for PM biosynthesis. Hence, we first looked for OGs with protein sequences from all five PM-containing archaea or from one Methanopyrales and three Methanobacteriales or from four Methanobacteriales. To identify OGs corresponding

to a widespread gene that would also include a paralogue potentially specific to PM-containing archaea, we used the same taxonomic criteria but set the 'min_copy_mean' option to 1.75 for PM-containing archaea and to 1.25 for other species (see YAML configuration files for details). In addition, three HMM profiles from NCBI CDD (Conserved Domain Database) (68) featuring 'pseudomurein' in their annotation were downloaded on December 18th, 2020. Then the profiles were used to identify homologues in the conceptual translations of the five PM-containing archaea with hmmsearch from the HMMER package v3.3 (92) with default parameters. Matching protein sequences were graphically selected using the Ompa-Pa v0.211430 interactive software package (A. Bertrand and D. Baurain; https://metacpan.org/dist/Bio-MUST-Apps-OmpaPa) with the 'max_copy' option set to 20 and 'min_cov' to 0.7. Finally, the corresponding OGs were added to the selection.

Genetic environment analysis of candidate proteins and *in silico* characterization of their domains

Genetic environment databases were built for the genes of the selected OGs using the "3 in 1" module of GeneSpy (93). Functional domains were predicted using InterProScan v5.37-76.0 (94), along with SignalP v5.0b (95) and TMHMM v2.0c (96). InterProScan was used with default parameters and we disabled the precalculated match lookup, while the SignalP organism option was set to 'arch'. To avoid misprediction by TMHMM, the signal peptide was first removed from the original sequences when the cleavage site prediction probability was greater than or equal to 0.1.

Filtering of candidate proteins

To rescue potential pseudogenes or mistranslated proteins missing in selected OGs with protein sequences from only four (out of five) PM-containing archaea, Forty-Two v0.213470 was run in TBLASTN mode on the whole genomic sequences of the five PM-containing archaea. Then, classify-ali.pl was used again to retain only the OGs having sequences from all five PM-containing archaea. To enrich OGs with further archaeal orthologues, a second round of forty-two.pl in BLASTP mode was

performed using the archaeal database of 819 whole genomes (see YAML configuration files for details). Each enriched OG was aligned using MAFFT L-INS-i v7.273 (97). From those alignments, HMM profiles were built using the HMMER package and bacterial homologues were identified separately in the bacterial and the prokaryotic databases. Protein sequences were graphically selected using Ompa-Pa with 'max_copy' and 'min_cov' options set to 20 and 0.7, respectively. For each OG, identical length and e-value thresholds were used for both databases when selecting homologous proteins.

Phylogenetic analyses

ATP-grasp superfamily

In order to select a set of representative sequences containing the ATP-grasp domain, we first built a HMM profile from the alignment of the OG containing archaeal ATP-grasp domain proteins using the HMMER package. This profile was uploaded to the HMMER website (https://www.ebi.ac.uk/Tools/hmmer/search/hmmsearch) from which we retrieved homologous sequences (excluding eukaryotes) from the Swiss-Prot database (98). From those sequences, homologues were identified in our local bacterial databases using the HMM profile and Ompa-Pa. In parallel, the archaeal OGs (see Identification of candidate proteins for pseudomurein biosynthesis) homologous to the Swiss-Prot proteins were identified using NCBI BLASTp v2.2.28+ (99) and enriched using Forty-Two with the archaeal database as 'bank'. Finally, all archaeal and bacterial homologous sequences were merged into one single file.

To identify most ATP-grasp-containing domain proteins in our local databases, the merged file was aligned using MAFFT L-INS-i and the alignment was masked using the mask-ali.pl perl script (D. Baurain; https://metacpan.org/dist/Bio-MUST-Core) to isolate the ATP-grasp domain. From this domain alignment, an HMM profile was built using the HMMER package to identify ATP-grasp domain-containing homologues in our archaeal and bacterial databases, and homologous sequences were selected using Ompa-Pa. Protein sequences with two ATP-grasp domains (i.e., CarB) were cut at half-length, then both complete and half-sequences were aligned using

MAFFT and their ATP-grasp domain again isolated using mask-ali.pl. Protein sequences were deduplicated using cdhit-tax-filter.pl perl script (V. Lupo and D. Baurain; https://metacpan.org/dist/Bio-MUST-Drivers) with the 'keep-all' option enabled and the identity threshold set to 0.65, then tagged using a BLAST-based annotation script (part of Bio-MUST-Drivers) and highly divergent sequences were removed using prune-outliers.pl v0.213470 with the 'evalue' option set to 1e-3, 'min-hits' to 1, 'min_ident' to 0.01 and 'max_ident' to 0.2. Finally, sequences were realigned with MAFFT L-INS-i. Conserved sites were selected using ali2phylip.pl v0.212670 (D. Baurain; https://metacpan.org/dist/Bio-MUST-Core) with the 'min' and 'max' options set to 0.3. The resulting matrix of 2,194 sequences x 180 AAs was used to infer phylogenetic domain trees using IQ-TREE v1.6.12 (100) with 1000 ultrafast bootstrap (UFBoot) replicates (101) and under four models: LG4X+R4, C20+G4, C40+G4 and PMSF LG+C60+G4. In total, seven trees were computed because we tested the effect of increasing the number of iterations from 1000 to 3000 for the C20 and C40 models, and from 3000 to 5000 for the PMSF model.

MraY-like family

The two OGs (see Identification of candidate proteins for pseudomurein biosynthesis) containing proteins predicted with a domain glycosyltransferase 4 were enriched in bacterial homologues using Forty-Two in BLASTP mode. In parallel, representative sequences from other members of the MraY-like family (https://www.ncbi.nlm.nih.gov/Structure/cdd/cddsrv.cgi?uid=264002) were downloaded from the UniProtKB (102) database: WecA (P0AC78, P0AC80, Q8Z38), GPT (P96000, B5IDH8) and WbpL (G3XD50, A0A379IBB8). The three files were then enriched in bacterial and archaeal (if any) homologues using Forty-Two. Finally, the five files were aligned using MAFFT L-INS-i.

To better explore the diversity of the MraY-like family, HMM profiles were built from those alignments and homologous sequences were selected from HMMER hits on the bacterial database using Ompa-Pa. All homologous protein sequences were merged into one file and tagged using a BLAST-based annotation script (part of Bio-MUST-Drivers) and aligned using MAFFT L-INS-i. Conserved sites were selected using ali2phylip.pl with the 'min' and 'max' options set to 0.2. A first guide tree was computed from the resulting matrix of 1070 sequences x 410 AAs using IQ-TREE

764 with 1000 UFBoot under the LG4X+R4 model. From this guide tree and automated
765 annotation, all sequences were manually tagged using 'treeplot' from the MUST
766 software package (103). According to their annotation, protein sequences of each
767 member of the MraY-like family were aligned using MAFFT L-INS-i, then all
768 members were realigned using Two-Scalp v0.211710 (A. Bertrand, V. Lupo and D.
769 Baurain; https://metacpan.org/dist/Bio-MUST-Apps-TwoScalp) with the 'linsi' option
770 enabled. Finally, ali2phylip.pl was used to select conserved sites with the 'min' and
771 'max' options set to 0.2 and the resulting matrix of 1070 sequences x 408 AAs was
772 used to infer phylogenetic trees with IQ-TREE under three models (i.e., LG4X+R4,
773 C20+G4, C40+G4) and 1000 UFBoot.

774 Mur domain-containing family

775 After enrichment of the OGs with archaeal and bacterial homologues, the multiple
776 OGs corresponding to the Mur domain-containing family were merged into one
777 single (unaligned) file. In parallel, reference protein sequences from additional
778 members of the Mur domain-containing family were downloaded into three separated
779 files using the command-line version of the 'efetch' tool v10.4 from the NCBI Entrez
780 Programming Utilities (E-utilities): CapB (P96736), MurT (Q8DNZ9, A0A0H3JUU7,
781 A0A0H2WZQ7) and CphA (P56947, O86109, P58572). Forty-Two in BLASTP mode
782 was run, in two rounds, on the four files, using both bacterial and archaeal databases
783 as 'bank', in a final effort to sample the diversity of Mur domain-containing proteins.
784 Then, fusion proteins were cut between the two protein domains and half-sequences
785 with no Mur ligase domain were discarded. The enriched files were merged and
786 protein sequences were deduplicated using the cdhit-tax-filter.pl with the 'keep-all'
787 option enabled and the identity threshold set to 1. Mur domain-containing family
788 proteins were tagged using a BLAST-based annotation script (part of Bio-MUST-
789 Drivers) with an e-value threshold of 1e-20. Protein sequences were aligned using
790 MAFFT (default mode) and conserved sites were selected using ali2phylip.pl with the
791 'max' option set to 0.3. A first guide tree was computed with IQ-TREE under the
792 LG4X+R4 model with 1000 UFBoot. Based on the automatic annotation, all protein
793 sequences were manually tagged following the guide tree using 'treeplot' from the
794 MUST software package.
795
796 In order to improve phylogenetic analysis, the alignment of the Mur domain-

containing family was refined as follows: 1) sequences from the different members of the family were exported to distinct files and aligned using MAFFT L-INS-i, 2) using the ‘ed’ programme from the MUST software package, misaligned sequences were manually transferred to a ‘.non’ file, and then, reduced files were realigned using MAFFT L-INS-i, 3) realigned files and ‘.non’ files were merged and all sequences were aligned using Two-Scalp with the ‘linsi’ and ‘keep-length’ options enabled. Conserved sites were selected using ali2phylip.pl with the ‘max’ and ‘min’ option set to 0.3. Phylogenetic analysis was performed on the resulting matrix of 3407 sequences x 550 AAs using IQ-TREE with 1000 UFBoot under three models of sequence evolution: LG4X+R4, C20+G4 and C40+G4.

The concatenated MurT/GatD tree was constructed as follows: first, three sequences of GatD (Q8DNZ8, A0A0H3JN63 and A0A0H2WZ38) were downloaded using ‘efetch’. Then, two rounds of Forty-Two in BLASTP mode were run, using both bacterial and archaeal local databases. In order to identify the orthologues of GatD, a preliminary tree was constructed using IQ-TREE with 1000 UFBoot under the LG4X+R4 model (data not shown). The non-deduplicated sequences (see above) identified as orthologues of MurT and GatD were concatenated and aligned using MAFFT with ‘auto’ and ‘reorder’ options enabled. Finally, conserved sites were selected using ali2phylip.pl with the ‘max’ option set to 0.8, and the resulting matrix of 229 sequences x 640 AAs was used to infer phylogenetic trees with IQ-TREE under the three usual models (i.e., LG4X+R4, C20+G4, C40+G4) with 1000 UFBoot.

The jackknife.pl perl script (part of Bio-MUST-Drivers) was used for species resampling analysis with the ‘linsi’ option enabled, ‘min’ and ‘max’ set to 0.3 and ‘n-process’ to 1000. The one thousand resulting alignments were used to infer phylogenetic trees using IQ-TREE with 1000 UFBoot under the LG4X+R4, C20+G4 and C40+G4 models. Clan support values were assessed using the parse_consense_out.pl perl script (104) with the ‘mode’ option set to ‘tree’. Consensus trees were computed from the 1000 replicate trees using ASTRAL v5.7.7 (105) with default options.

Acknowledgements

VL is supported by a FRIA (Fonds pour la Formation à la Recherche dans l'Industrie et dans l'Agriculture) fellowship of the F.R.S.-FNRS. FK is a research associate of the F.R.S.-FNRS. Computational resources were provided through two grants to DB (University of Liège “Crédit de démarrage 2012” SFRD-12/04; F.R.S.-FNRS “Crédit de recherche 2014” CDR J.0080.15), and by the Consortium des Équipements de Calcul Intensif (CÉCI) funded by the F.R.S.-FNRS.

Authors’ Contributions

VL conceived the study and designed experiments, performed experiments, analyzed the data, drafted and drew the figures, wrote the manuscript and approved the final manuscript. DB conceived the study and designed experiments, analyzed the data, wrote and reviewed the manuscript and approved the final manuscript. FK conceived the study, analyzed the data, reviewed the manuscript and approved the final manuscript. CR, ER, LO, OJ, and CM performed experiments and approved the final manuscript.

References

1. Pazos M, Peters K. 2019. Peptidoglycan, p. 127–168. *In* Kuhn, A (ed.), Bacterial Cell Walls and Membranes. Springer International Publishing, Cham.
2. Meyer BH, Albers S-V. 2020. Archaeal Cell Walls, p. 1–14. *In* eLS.
3. Rodrigues-Oliveira T, Belmok A, Vasconcellos D, Schuster B, Kyaw CM. 2017. Archaeal S-Layers: Overview and Current State of the Art. Front Microbiol 8:2597.
4. Albers S-V, Meyer BH. 2011. The archaeal cell envelope. Nat Rev Microbiol 9:414–426.
5. Vollmer W, Blanot D, de Pedro MA. 2008. Peptidoglycan structure and architecture. FEMS Microbiol Rev 32:149–167.
6. König H, Kralik R, Kandler O. 1982. Structure and Modifications of Pseudomurein in Methano-bacleriales. Zentralblatt Für Bakteriol Mikrobiol Hyg Abt Orig C Allg Angew

Ökol Mikrobiol 3:179–191.

7. König H, Hartmann E, Kärcher U. 1993. Pathways and Principles of the Biosynthesis of Methanobacterial Cell Wall Polymers. Syst Appl Microbiol 16:510–517.

8. Hartmann E, König H. 1990. Comparison of the biosynthesis of the methanobacterial pseudomurein and the eubacterial murein. Naturwissenschaften 77:472–475.

9. Hartmann E, König H. 1994. A novel pathway of peptide biosynthesis found in methanogenic Archaea. Arch Microbiol 162:430–432.

10. Kandler O, Konig H. 1993. Chapter 8 Cell envelopes of archaea: Structure and chemistry, p. 223–259. *In* Kates, M, Kushner, DJ, Matheson, AT (eds.), New Comprehensive Biochemistry. Elsevier.

11. Scheffers D-J, Pinho MG. 2005. Bacterial cell wall synthesis: new insights from localization studies. Microbiol Mol Biol Rev MMBR 69:585–607.

12. Bapteste E, Brochier C, Boucher Y. 2005. Higher-level classification of the Archaea: evolution of methanogenesis and methanogens. Archaea Vanc BC 1:353–363.

13. Williams TA, Cox CJ, Foster PG, Szöllősi GJ, Embley TM. 2020. Phylogenomics provides robust support for a two-domains tree of life. Nat Ecol Evol 4:138–147.

14. Aouad M, Flandrois J-P, Jauffrit F, Gouy M, Gribaldo S, Brochier-Armanet C. 2022. A divide-and-conquer phylogenomic approach based on character supermatrices resolves early steps in the evolution of the Archaea. BMC Ecol Evol 22:1.

15. Gribaldo S, Brochier-Armanet C, Gribaldo S, Brochier-Armanet C. 2006. The origin and evolution of Archaea: a state of the art. Philos Trans R Soc Lond B Biol Sci 361:1007–1022.

16. Da Cunha V, Gaia M, Nasir A, Forterre P. 2018. Asgard archaea do not close the debate about the universal tree of life topology. PLoS Genet 14:e1007215.

17. Liechti GW, Kuru E, Hall E, Kalinda A, Brun YV, VanNieuwenhze M, Maurelli AT. 2014. A new metabolic cell-wall labelling method reveals peptidoglycan in Chlamydia trachomatis. Nature 506:507–510.

18. Jeske O, Schüler M, Schumann P, Schneider A, Boedeker C, Jogler M, Bollschweiler

D, Rohde M, Mayer C, Engelhardt H, Spring S, Jogler C. 2015. Planctomycetes do possess a peptidoglycan cell wall. Nat Commun 6:7116.

19. Packiam M, Weinrick B, Jacobs WRJ, Maurelli AT. 2015. Structural characterization of muropeptides from Chlamydia trachomatis peptidoglycan by mass spectrometry resolves “chlamydial anomaly”. Proc Natl Acad Sci U S A 112:11660–11665.

20. van Teeseling MCF, Mesman RJ, Kuru E, Espaillat A, Cava F, Brun YV, VanNieuwenhze MS, Kartal B, van Niftrik L. 2015. Anammox Planctomycetes have a peptidoglycan cell wall. Nat Commun 6:6878.

21. Liechti G, Kuru E, Packiam M, Hsu Y-P, Tekkam S, Hall E, Rittichier JT, VanNieuwenhze M, Brun YV, Maurelli AT. 2016. Pathogenic Chlamydia Lack a Classical Sacculus but Synthesize a Narrow, Mid-cell Peptidoglycan Ring, Regulated by MreB, for Cell Division. PLoS Pathog 12:e1005590.

22. Bhattacharjee MK. 2016. Antibiotics That Inhibit Cell Wall Synthesis, p. 49–94. *In* Bhattacharjee, MK (ed.), Chemistry of Antibiotics and Related Drugs. Springer International Publishing, Cham.

23. Tamames J. 2001. Evolution of gene order conservation in prokaryotes. Genome Biol 2:RESEARCH0020.

24. Mingorance J, Tamames J. 2004. The bacterial dcw gene cluster: an island in the genome?, p. 249–271. *In* Vicente, M, Tamames, J, Valencia, A, Mingorance, J (eds.), Molecules in Time and Space: Bacterial Shape, Division and Phylogeny. Springer US, Boston, MA.

25. Real G, Henriques AO. 2006. Localization of the Bacillus subtilis murB gene within the dcw cluster is important for growth and sporulation. J Bacteriol 188:1721–1732.

26. Pilhofer M, Rappl K, Eckl C, Bauer AP, Ludwig W, Schleifer K-H, Petroni G. 2008. Characterization and evolution of cell division and cell wall synthesis genes in the bacterial phyla Verrucomicrobia, Lentisphaerae, Chlamydiae, and Planctomycetes and phylogenetic comparison with rRNA genes. J Bacteriol 190:3192–3202.

27. Martínez-Torró C, Torres-Puig S, Marcos-Silva M, Huguet-Ramón M, Muñoz-Navarro

C, Lluch-Senar M, Serrano L, Querol E, Piñol J, Pich OQ. 2021. Functional Characterization of the Cell Division Gene Cluster of the Wall-less Bacterium Mycoplasma genitalium. Front Microbiol 12:695572.

28. Léonard RR, Sauvage E, Lupo V, Perrin A, Sirjacobs D, Charlier P, Kerff F, Baurain D. 2022. Was the Last Bacterial Common Ancestor a Monoderm after All? Genes 13:376.

29. Egan AJF, Errington J, Vollmer W. 2020. Regulation of peptidoglycan synthesis and remodelling. Nat Rev Microbiol 18:446–460.

30. Zawadzke LE, Norcia M, Desbonnet CR, Wang H, Freeman-Cook K, Dougherty TJ. 2008. Identification of an inhibitor of the MurC enzyme, which catalyzes an essential step in the peptidoglycan precursor synthesis pathway. Assay Drug Dev Technol 6:95–103.

31. Kouidmi I, Levesque RC, Paradis-Bleau C. 2014. The biology of Mur ligases as an antibacterial target. Mol Microbiol 94:242–253.

32. Münch D, Roemer T, Lee SH, Engeser M, Sahl HG, Schneider T. 2012. Identification and in vitro analysis of the GatD/MurT enzyme-complex catalyzing lipid II amidation in Staphylococcus aureus. PLoS Pathog 8:e1002509.

33. Nöldeke ER, Muckenfuss LM, Niemann V, Müller A, Störk E, Zocher G, Schneider T, Stehle T. 2018. Structural basis of cell wall peptidoglycan amidation by the GatD/MurT complex of Staphylococcus aureus. Sci Rep 8:12953.

34. Makino S, Uchida I, Terakado N, Sasakawa C, Yoshikawa M. 1989. Molecular characterization and protein analysis of the cap region, which is essential for encapsulation in Bacillus anthracis. J Bacteriol 171:722–730.

35. Ashiuchi M. 2013. Microbial production and chemical transformation of poly-γ-glutamate. Microb Biotechnol 6:664–674.

36. Hsueh Y-H, Huang K-Y, Kunene SC, Lee T-Y. 2017. Poly-γ-glutamic Acid Synthesis, Gene Regulation, Phylogenetic Relationships, and Role in Fermentation. Int J Mol Sci 18:2644.

37. Aboulmagd E, Oppermann-Sanio FB, Steinbüchel A. 2001. Purification of Synechocystis sp. strain PCC6308 cyanophycin synthetase and its characterization with respect to substrate and primer specificity. Appl Environ Microbiol 67:2176–2182.

38. Sharon I, Haque AS, Grogg M, Lahiri I, Seebach D, Leschziner AE, Hilvert D, Schmeing TM. 2021. Structures and function of the amino acid polymerase cyanophycin synthetase. Nat Chem Biol 17:1101–1110.

39. Levin I, Giladi M, Altman-Price N, Ortenberg R, Mevarech M. 2004. An alternative pathway for reduced folate biosynthesis in bacteria and halophilic archaea. Mol Microbiol 54:1307–1318.

40. Gorelova V, Bastien O, De Clerck O, Lespinats S, Rébeillé F, Van Der Straeten D. 2019. Evolution of folate biosynthesis and metabolism across algae and land plant lineages. Sci Rep 9:5731.

41. Kordus SL, Baughn AD. 2019. Revitalizing antifolates through understanding mechanisms that govern susceptibility and resistance. MedChemComm 10:880–895.

42. Fawaz MV, Topper ME, Firestine SM. 2011. The ATP-grasp enzymes. Bioorganic Chem 39:185–191.

43. Shi D, Caldovic L, Tuchman M. 2018. Sources and Fates of Carbamyl Phosphate: A Labile Energy-Rich Molecule with Multiple Facets. Biology 7:34.

44. Lawson FS, Charlebois RL, Dillon JA. 1996. Phylogenetic analysis of carbamoylphosphate synthetase genes: complex evolutionary history includes an internal duplication within a gene which can root the tree of life. Mol Biol Evol 13:970–977.

45. Philippe H, Forterre P. 1999. The rooting of the universal tree of life is not reliable. J Mol Evol 49:509–523.

46. Cammarano P, Gribaldo S, Johann A. 2002. Updating carbamoylphosphate synthase (CPS) phylogenies: occurrence and phylogenetic identity of archaeal CPS genes. J Mol Evol 55:153–160.

47. Smith DR, Doucette-Stamm LA, Deloughery C, Lee H, Dubois J, Aldredge T,

Bashirzadeh R, Blakely D, Cook R, Gilbert K, Harrison D, Hoang L, Keagle P, Lumm W, Pothier B, Qiu D, Spadafora R, Vicaire R, Wang Y, Wierzbowski J, Gibson R, Jiwani N, Caruso A, Bush D, Reeve JN. 1997. Complete genome sequence of Methanobacterium thermoautotrophicum deltaH: functional analysis and comparative genomics. J Bacteriol 179:7135–7155.

48. Slesarev AI, Mezhevaya KV, Makarova KS, Polushin NN, Shcherbinina OV, Shakhova VV, Belova GI, Aravind L, Natale DA, Rogozin IB, Tatusov RL, Wolf YI, Stetter KO, Malykh AG, Koonin EV, Kozyavkin SA. 2002. The complete genome of hyperthermophile Methanopyrus kandleri AV19 and monophyly of archaeal methanogens. Proc Natl Acad Sci U S A 99:4644–4649.

49. Samuel BS, Hansen EE, Manchester JK, Coutinho PM, Henrissat B, Fulton R, Latreille P, Kim K, Wilson RK, Gordon JI. 2007. Genomic and metabolic adaptations of Methanobrevibacter smithii to the human gut. Proc Natl Acad Sci U S A 104:10643–10648.

50. Leahy SC, Kelly WJ, Altermann E, Ronimus RS, Yeoman CJ, Pacheco DM, Li D, Kong Z, McTavish S, Sang C, Lambie SC, Janssen PH, Dey D, Attwood GT. 2010. The genome sequence of the rumen methanogen Methanobrevibacter ruminantium reveals new possibilities for controlling ruminant methane emissions. PloS One 5:e8926.

51. Graham DE, Huse HK. 2008. Methanogens with pseudomurein use diaminopimelate aminotransferase in lysine biosynthesis. FEBS Lett 582:1369–1374.

52. Subedi BP, Martin WF, Carbone V, Duin EC, Cronin B, Sauter J, Schofield LR, Sutherland-Smith AJ, Ronimus RS. 2021. Archaeal pseudomurein and bacterial murein cell wall biosynthesis share a common evolutionary ancestry. FEMS Microbes 2:xtab012.

53. Ithurbide S, Gribaldo S, Albers S-V, Pende N. 2022. Spotlight on FtsZ-based cell division in Archaea. Trends Microbiol 30:665–678.

54. Subedi BP, Schofield LR, Carbone V, Wolf M, Martin WF, Ronimus RS, Sutherland-

Smith AJ. 2022. Structural characterisation of methanogen pseudomurein cell wall peptide ligases homologous to bacterial MurE/F murein peptide ligases. Microbiology,. Microbiology Society, 001235.

55. Braun F, Recalde A, Bähre H, Seifert R, Albers S-V. 2021. Putative Nucleotide-Based Second Messengers in the Archaeal Model Organisms Haloferax volcanii and Sulfolobus acidocaldarius. Front Microbiol 12:779012.

56. Chen H, Gan Q, Fan C. 2020. Methyl-Coenzyme M Reductase and Its Post-translational Modifications. Front Microbiol 11:578356.

57. Popa E, Perera N, Kibédi-Szabó CZ, Guy-Evans H, Evans DR, Purcarea C. 2012. The smallest active carbamoyl phosphate synthetase was identified in the human gut archaeon Methanobrevibacter smithii. J Mol Microbiol Biotechnol 22:287–299.

58. Cristianini N, Hahn MW. 2006. Introduction to Computational Genomics: A Case Studies Approach. Cambridge University Press. https://books.google.be/books?id=t3lkngEACAAJ.

59. Anderssen S, Naômé A, Jadot C, Brans A, Tocquin P, Rigali S. 2022. AURTHO: Autoregulation of transcription factors as facilitator of cis-acting element discovery. Biochim Biophys Acta BBA - Gene Regul Mech 1865:194847.

60. Diesterhaft MD, Freese E. 1973. Role of pyruvate carboxylase, phosphoenolpyruvate carboxykinase, and malic enzyme during growth and sporulation of Bacillus subtilis. J Biol Chem 248:6062–6070.

61. Shen Y, Chou C-Y, Chang G-G, Tong L. 2006. Is dimerization required for the catalytic activity of bacterial biotin carboxylase? Mol Cell 22:807–818.

62. Hou J, Xiang H, Han J. 2015. Propionyl coenzyme A (propionyl-CoA) carboxylase in Haloferax mediterranei: Indispensability for propionyl-CoA assimilation and impacts on global metabolism. Appl Environ Microbiol 81:794–804.

63. Mueller EJ, Meyer E, Rudolph J, Davisson VJ, Stubbe J. 1994. N5-carboxyaminoimidazole ribonucleotide: evidence for a new intermediate and two new enzymatic activities in the de novo purine biosynthetic pathway of Escherichia coli.

Biochemistry 33:2269–2278.

64. Marolewski AE, Mattia KM, Warren MS, Benkovic SJ. 1997. Formyl phosphate: a proposed intermediate in the reaction catalyzed by Escherichia coli PurT GAR transformylase. Biochemistry 36:6709–6716.

65. Musfeldt M, Schönheit P. 2002. Novel Type of ADP-Forming Acetyl Coenzyme A Synthetase in Hyperthermophilic *Archaea*: Heterologous Expression and Characterization of Isoenzymes from the Sulfate Reducer *Archaeoglobus fulgidus* and the Methanogen *Methanococcus jannaschii*. J Bacteriol 184:636–644.

66. Joyce MA, Fraser ME, Brownie ER, James MN, Bridger WA, Wolodko WT. 1999. Probing the nucleotide-binding site of Escherichia coli succinyl-CoA synthetase. Biochemistry 38:7273–7283.

67. Cheng YS, Shen Y, Rudolph J, Stern M, Stubbe J, Flannigan KA, Smith JM. 1990. Glycinamide ribonucleotide synthetase from Escherichia coli: cloning, overproduction, sequencing, isolation, and characterization. Biochemistry 29:218–227.

68. Lu S, Wang J, Chitsaz F, Derbyshire MK, Geer RC, Gonzales NR, Gwadz M, Hurwitz DI, Marchler GH, Song JS, Thanki N, Yamashita RA, Yang M, Zhang D, Zheng C, Lanczycki CJ, Marchler-Bauer A. 2020. CDD/SPARCLE: the conserved domain database in 2020. Nucleic Acids Res 48:D265–D268.

69. Amer AO, Valvano MA. 2001. Conserved amino acid residues found in a predicted cytosolic domain of the lipopolysaccharide biosynthetic protein WecA are implicated in the recognition of UDP-N-acetylglucosamine. Microbiol Read Engl 147:3015–3025.

70. Campbell JA, Davies GJ, Bulone V, Henrissat B. 1997. A classification of nucleotide-diphospho-sugar glycosyltransferases based on amino acid sequence similarities. Biochem J 326 (Pt 3):929–939.

71. Price NP, Momany FA. 2005. Modeling bacterial UDP-HexNAc: polyprenol-P HexNAc-1-P transferases. Glycobiology 15:29R-42R.

72. Dal Nogare AR, Dan N, Lehrman MA. 1998. Conserved sequences in enzymes of the UDP-GlcNAc/MurNAc family are essential in hamster UDP-GlcNAc:dolichol-P

GlcNAc-1-P transferase. Glycobiology 8:625–632.

73. Lupo V, Van Vlierberghe M, Vanderschuren H, Kerff F, Baurain D, Cornet L. 2021. Contamination in Reference Sequence Databases: Time for Divide-and-Rule Tactics. Front Microbiol 12:755101.

74. Morlot C, Straume D, Peters K, Hegnar OA, Simon N, Villard A-M, Contreras-Martel C, Leisico F, Breukink E, Gravier-Pelletier C, Le Corre L, Vollmer W, Pietrancosta N, Håvarstein LS, Zapun A. 2018. Structure of the essential peptidoglycan amidotransferase MurT/GatD complex from Streptococcus pneumoniae. Nat Commun 9:3180.

75. Griffin M, Casadio R, Bergamini CM. 2002. Transglutaminases: nature's biological glues. Biochem J 368:377–396.

76. Gouy R, Baurain D, Philippe H. 2015. Rooting the tree of life: the phylogenetic jury is still out. Philos Trans R Soc B Biol Sci 370:20140329.

77. Laddomada F, Miyachiro MM, Jessop M, Patin D, Job V, Mengin-Lecreulx D, Le Roy A, Ebel C, Breyton C, Gutsche I, Dessen A. 2019. The MurG glycosyltransferase provides an oligomeric scaffold for the cytoplasmic steps of peptidoglycan biosynthesis in the human pathogen Bordetella pertussis. Sci Rep 9:4656.

78. Smith CA. 2006. Structure, function and dynamics in the mur family of bacterial cell wall ligases. J Mol Biol 362:640–655.

79. Díaz-Mejía JJ, Pérez-Rueda E, Segovia L. 2007. A network perspective on the evolution of metabolism by gene duplication. Genome Biol 8:R26.

80. Sato N. 2021. Are Cyanobacteria an Ancestor of Chloroplasts or Just One of the Gene Donors for Plants and Algae? Genes 12.

81. Ponce-Toledo RI, López-García P, Moreira D. 2019. Horizontal and endosymbiotic gene transfer in early plastid evolution. New Phytol 224:618–624.

82. Maitra A, Nukala S, Dickman R, Martin LT, Munshi T, Gupta A, Shepherd AJ, Arnvig KB, Tabor AB, Keep NH, Bhakta S. 2021. Characterization of the MurT/GatD complex in Mycobacterium tuberculosis towards validating a novel anti-tubercular drug target.

JAC-Antimicrob Resist 3:dlab028.

83. Beaud Benyahia B, Taib N, Beloin C, Gribaldo S. 2024. Terrabacteria: redefining bacterial envelope diversity, biogenesis and evolution. Nat Rev Microbiol https://doi.org/10.1038/s41579-024-01088-0.

84. Mengin-Lecreulx D, Texier L, Rousseau M, van Heijenoort J. 1991. The murG gene of Escherichia coli codes for the UDP-N-acetylglucosamine: N-acetylmuramyl-(pentapeptide) pyrophosphoryl-undecaprenol N-acetylglucosamine transferase involved in the membrane steps of peptidoglycan synthesis. J Bacteriol 173:4625–4636.

85. Lombard V, Golaconda Ramulu H, Drula E, Coutinho PM, Henrissat B. 2014. The carbohydrate-active enzymes database (CAZy) in 2013. Nucleic Acids Res 42:D490-495.

86. Walker MC, van der Donk WA. 2016. The many roles of glutamate in metabolism. J Ind Microbiol Biotechnol 43:419–430.

87. Irisarri I, Baurain D, Brinkmann H, Delsuc F, Sire J-Y, Kupfer A, Petersen J, Jarek M, Meyer A, Vences M. 2017. Phylotranscriptomic consolidation of the jawed vertebrate timetree. Nat Ecol Evol 1:1370–1378.

88. Simion P, Philippe H, Baurain D, Jager M, Richter DJ, Di Franco A, Roure B, Satoh N, Quéinnec É, Ereskovsky A, Lapébie P, Corre E, Delsuc F, King N, Wörheide G, Manuel M. 2017. A Large and Consistent Phylogenomic Dataset Supports Sponges as the Sister Group to All Other Animals. Curr Biol CB 27:958–967.

89. Léonard RR, Leleu M, Vlierberghe MV, Cornet L, Kerff F, Baurain D. 2021. ToRQuEMaDA: tool for retrieving queried Eubacteria, metadata and dereplicating assemblies. PeerJ 9:e11348.

90. Lupo V, Mercuri PS, Frère J-M, Joris B, Galleni M, Baurain D, Kerff F. 2022. An Extended Reservoir of Class-D Beta-Lactamases in Non-Clinical Bacterial Strains. Microbiol Spectr 10:e0031522.

91. Emms DM, Kelly S. 2015. OrthoFinder: solving fundamental biases in whole genome

comparisons dramatically improves orthogroup inference accuracy. Genome Biol 16:157.

92. Mistry J, Finn RD, Eddy SR, Bateman A, Punta M. 2013. Challenges in homology search: HMMER3 and convergent evolution of coiled-coil regions. Nucleic Acids Res 41:e121.

93. Garcia PS, Jauffrit F, Grangeasse C, Brochier-Armanet C. 2019. GeneSpy, a user-friendly and flexible genomic context visualizer. Bioinformatics 35:329–331.

94. Jones P, Binns D, Chang H-Y, Fraser M, Li W, McAnulla C, McWilliam H, Maslen J, Mitchell A, Nuka G, Pesseat S, Quinn AF, Sangrador-Vegas A, Scheremetjew M, Yong S-Y, Lopez R, Hunter S. 2014. InterProScan 5: genome-scale protein function classification. Bioinformatics 30:1236–1240.

95. Almagro Armenteros JJ, Tsirigos KD, Sønderby CK, Petersen TN, Winther O, Brunak S, von Heijne G, Nielsen H. 2019. SignalP 5.0 improves signal peptide predictions using deep neural networks. Nat Biotechnol 37:420–423.

96. Krogh A, Larsson B, von Heijne G, Sonnhammer EL. 2001. Predicting transmembrane protein topology with a hidden Markov model: application to complete genomes. J Mol Biol 305:567–580.

97. Katoh K, Standley DM. 2013. MAFFT multiple sequence alignment software version 7: improvements in performance and usability. Mol Biol Evol 30:772–780.

98. Poux S, Arighi CN, Magrane M, Bateman A, Wei C-H, Lu Z, Boutet E, Bye-A-Jee H, Famiglietti ML, Roechert B, UniProt Consortium T. 2017. On expert curation and scalability: UniProtKB/Swiss-Prot as a case study. Bioinforma Oxf Engl 33:3454–3460.

99. Camacho C, Coulouris G, Avagyan V, Ma N, Papadopoulos J, Bealer K, Madden TL. 2009. BLAST+: architecture and applications. BMC Bioinformatics 10:421.

100. Nguyen L-T, Schmidt HA, von Haeseler A, Minh BQ. 2015. IQ-TREE: a fast and effective stochastic algorithm for estimating maximum-likelihood phylogenies. Mol Biol Evol 32:268–274.

101. Hoang DT, Chernomor O, von Haeseler A, Minh BQ, Vinh LS. 2018. UFBoot2: Improving the Ultrafast Bootstrap Approximation. Mol Biol Evol 35:518–522.

102. The UniProt Consortium. 2021. UniProt: the universal protein knowledgebase in 2021. Nucleic Acids Res 49:D480–D489.

103. Philippe H. 1993. MUST, a computer package of Management Utilities for Sequences and Trees. Nucleic Acids Res 21:5264–5272.

104. Baurain D, Brinkmann H, Petersen J, Rodríguez-Ezpeleta N, Stechmann A, Demoulin V, Roger AJ, Burger G, Lang BF, Philippe H. 2010. Phylogenomic Evidence for Separate Acquisition of Plastids in Cryptophytes, Haptophytes, and Stramenopiles. Mol Biol Evol 27:1698–1709.

105. Zhang C, Rabiee M, Sayyari E, Mirarab S. 2018. ASTRAL-III: polynomial time species tree reconstruction from partially resolved gene trees. BMC Bioinformatics 19:153.

Table 1. Overview of the proteins identified in our pangenomic search for genes involved in PM biosynthesis. Orthologous Groups (OGs) composing the identified gene clusters, named clusters A to E are listed. For each OG, there is the functional prediction of InterProScan (if any), the predicted signal peptide type (SP) and the number of predicted transmembrane (TM) segments (0 = cytoplasmic, 1 = monotopic, >1 = polytopic).

Cluster	Orthologous Groups	InterProScan Prediction	Signal peptide	# TM
A	OG0001014	CPS large subunit, ATP-grasp	Other	0
	OG0001163	MraY-like	Other	>1
	OG0001473	Muramyl ligase (= Murδ)	Other	0
	OG0001162	/	Sec	0
	OG0001472	/	Other	1
	OG0000796	/	Other	>1

B	OG0001150	Muramyl ligase (= Murγ)	Other	0
	OG0001147	/	Other	0
	OG0001146	MobA-like NTP transferase domain	Other	0
	OG0000169	/	Sec	0
A-B	OG0001148	Muramyl ligase (= Murα)	Other	0
	OG0001149	Muramyl ligase (= Murß)	Other	0
C	OG0001210	Aminotransferases class-I pyridoxal-phosphate attachment site	Other	0
	OG0000094	MreB/DnaK-like	Other	0
	OG0001176	Coiled coil protein	Other	0
	OG0001177	Flp pilus assembly protein RcpC/CpaB	Other	1
	OG0001178	Sortase E	Other	>1
D	OG0001213	Zc3h12a-like Ribonuclease NYN domain	Other	0
	OG0001214	Nucleotide cyclase	Other	>1
E	OG0000266	Methyl-coenzyme M reductase, beta subunit	Other	0
	OG0000231	Methyl-coenzyme M reductase operon protein D	Other	0
	OG0000230	Methyl-coenzyme M reductase, gamma subunit	Other	0
	OG0000229	Methyl-coenzyme M reductase, alpha subunit	Other	0

Figure 1. Taxonomic distribution patterns of the 49 retained orthologous groups (OGs). The four OGs OG0001148, OG0001149, OG0001150 and OG0001473 are considered together and referred to as Muraßγδ and OG0001163 as MraY-like. Black lines delineate gene clusters in the genomes of PM-containing

archaea (clusters A to E). Full circle = gene present in the taxonomic group; empty circle = gene absent from the taxonomic group.

Figure 2. Phylogenetic tree of the ATP-grasp superfamily rooted on CarB. The tree was inferred from a matrix of 2,194 sequences x 180 unambiguously aligned AAs using IQ-TREE under the LG4X+R4 model. Tree visualization was performed using iTOL. Bootstrap support values are shown if greater or equal to 50%. Branches were collapsed on sequence annotation based on reference sequences. Black collapsed branches correspond to unannotated sequences.

Figure 3. Unrooted phylogenetic tree of the MraY-like family. The tree was constructed from a matrix of 1,070 sequences x 408 unambiguously aligned AAs using IQ-TREE under the C40+G4 model. Open circles correspond to bootstrap support values under 90%. Blue sequences correspond to a MraY annotation, green to WecA/WbpL, red to OG0001163 (MraY-like), yellow to OG0001207, purple to GPT, and black to unannotated bacterial sequences.

Figure 4. Phylogenetic trees of the Mur domain-containing family rooted on FPGS. (**a**) The tree was inferred from a matrix of 3,046 sequences x 543 unambiguously aligned AAs using IQ-TREE under the C40+G4 model. (**b**) **ASTRAL tree** computed **from the 1,000 C40+G4 species resampling trees**. Tree visualization was performed using iTOL. Support values are shown if greater or equal to 50% (**a**: bootstrap proportion; **b**: quartet support value). Branches were collapsed on identical sequence annotation, and to do so, two divergent sequences, one annotated as a MurE and the other as a MurF, were considered as CphA.

Figure 5. Phylogenetic tree of the concatenation of MurT/GatD rooted on the largest Bacillota clan. The tree was inferred from a matrix of 229 sequences x 653 unambiguously aligned AAs using IQ-TREE under the C40+G4 model. Tree visualization was performed using iTOL. Bootstrap support values are shown if greater or equal to 50%. Branches were collapsed based on taxonomic clans.

Figure 6. Evolutionary scenarios for the origins of the main Mur-domain containing genes in Archaea and Bacteria. (A-D) were theoretically possible but

are ruled out by the phylogenetic analyses performed in this study, whereas (E) is the most precise hypothesis that can be proposed in the current state of knowledge. A) LUCA possessed a single *mur* gene vertically inherited by both Archaea and Bacteria, and then independently duplicated (events d) thrice in each domain. B) LUCA was already carrying two paralogous *mur* genes, each one experiencing an additional duplication after their vertical transmission to both Archaea and Bacteria. C) All four *mur* genes were already existing in LUCA and were vertically transmitted to both Archaea and Bacteria. Alternatively, these four *mur* genes were only present in the LBCA and were each horizontally transferred (events t_1 to t_4) to (PM-containing) Archaea. D) The LBCA possessed the four *mur* genes and any of these (or even one of their ancestors) was horizontally transferred (event t_a, t_b or t_c) to (PM-containing) Archaea, where it experienced three duplications. E) As in D, the LBCA possessed the four *mur* genes, but only two of them were horizontally transferred (events t_1 and t_2) to (PM-containing) Archaea, in which one was duplicated twice. In detail, *murC* gave rise to *murδ*, whereas *murD* led to *muraßγ*. Moreover, an independant duplication (d*) of *murD* in Terrabacteria yielded *murT*, which was then horizontally transferred to (PM-containing) Archaea. (†) mur*α* is called pMurC in Subedi et al. (2021) (‡) mur*δ* is called pMurE in Subedi et al. (2022).

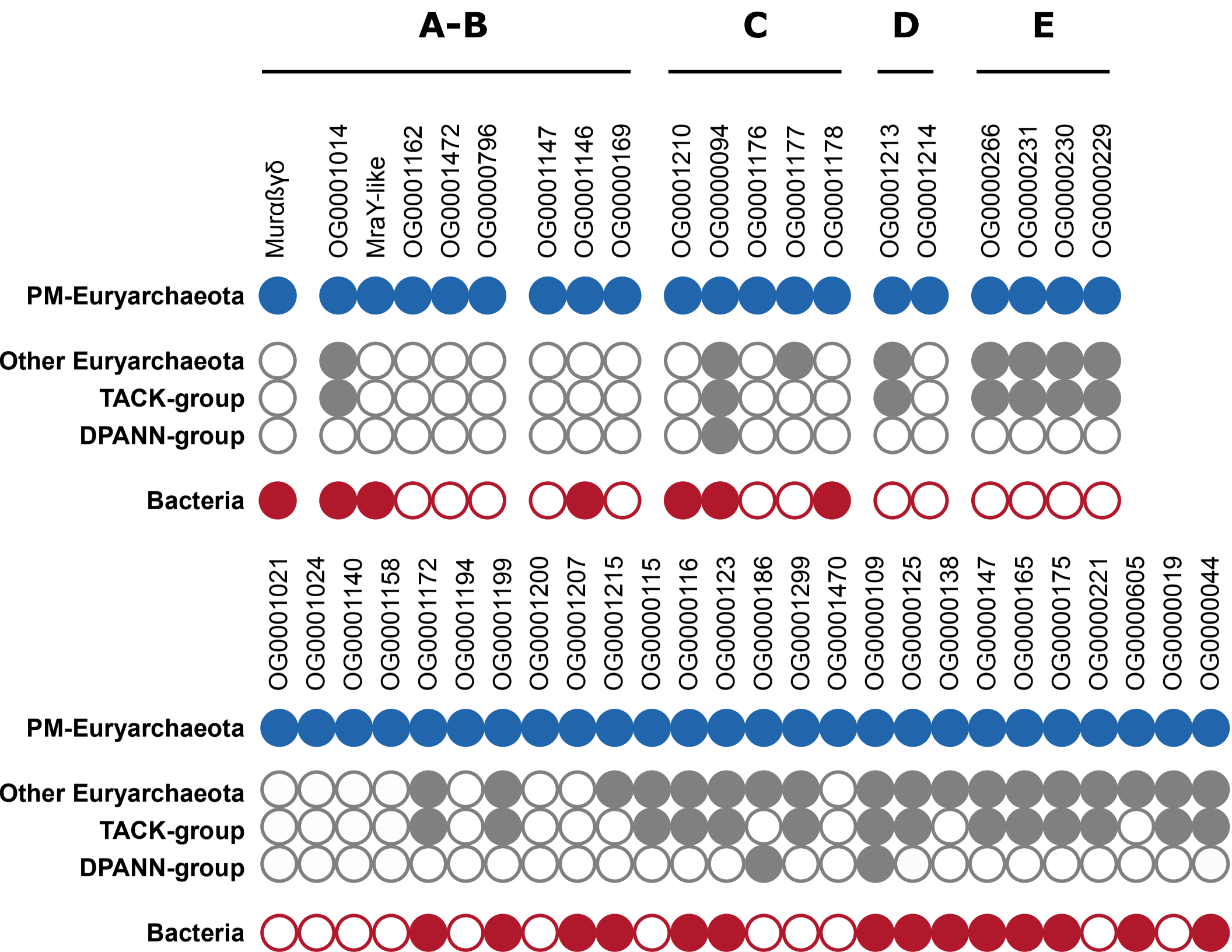
A-B
C
D
E
MuraßγΔ
OG0001014
MraY-like
OG0001162
OG0001472
OG0000796
OG0001147
OG0001146
OG0000169
OG0001210
OG0000094
OG0001176
OG0001177
OG0001178
OG0001213
OG0001214
OG0000266
OG0000231
OG0000230
OG0000229
PM-Euryarchaeota
Other Euryarchaeota
TACK-group
DPANN-group
Bacteria
OG0001021
OG0001024
OG0001140
OG0001158
OG0001172
OG0001194
OG0001199
OG0001200
OG0001207
OG0001215
OG0000115
OG0000116
OG0000123
OG0000186
OG0001299
OG0001470
OG0000109
OG0000125
OG0000138
OG0000147
OG0000165
OG0000175
OG0000221
OG0000605
OG0000019
OG0000044
PM-Euryarchaeota
Other Euryarchaeota
TACK-group
DPANN-group
Bacteria

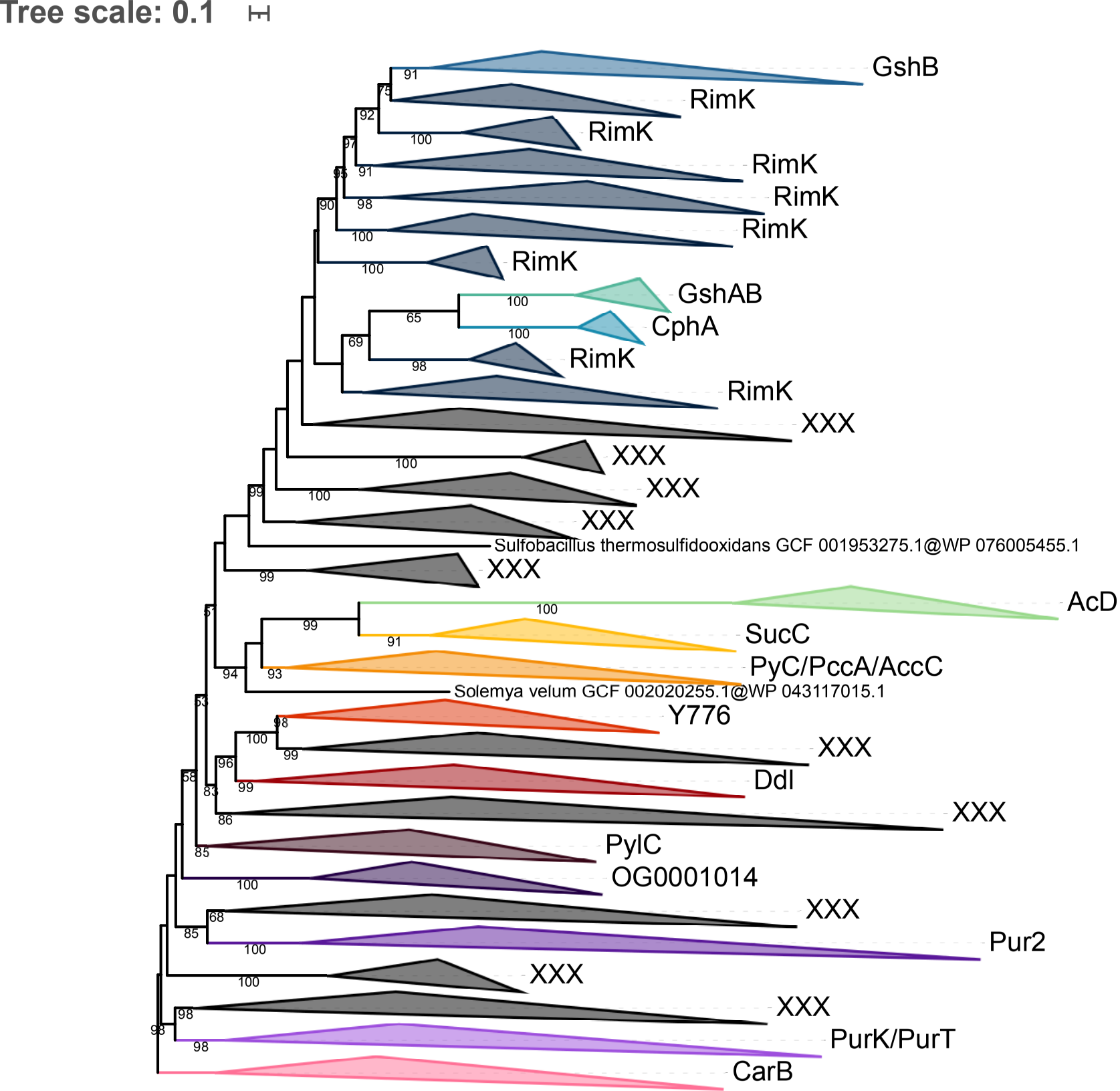
Tree scale: 0.1
GshB
RimK
RimK
RimK
RimK
RimK
RimK
GshAB
CphA
RimK
RimK
XXX
XXX
XXX
XXX
Sulfobacillus thermosulfidooxidans GCF 001953275.1@WP 076005455.1
XXX
AcD
SucC
PyC/PccA/AccC
Solemya velum GCF 002020255.1@WP 043117015.1
Y776
XXX
Ddl
XXX
PylC
OG0001014
XXX
Pur2
XXX
XXX
PurK/PurT
CarB

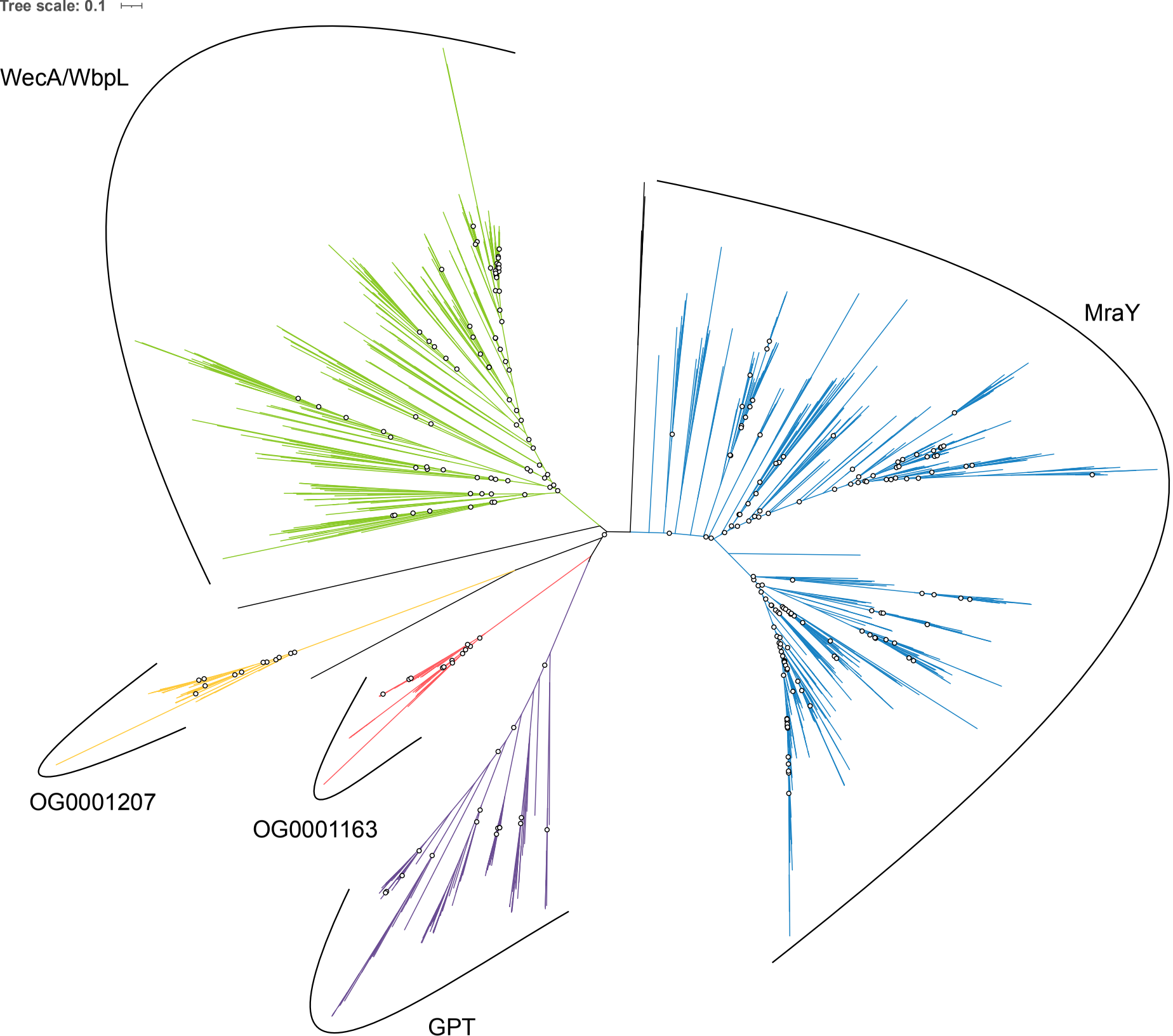
Tree scale: 0.1
WecA/WbpL
MraY
OG0001207
OG0001163
GPT

a

Tree scale: 0.1

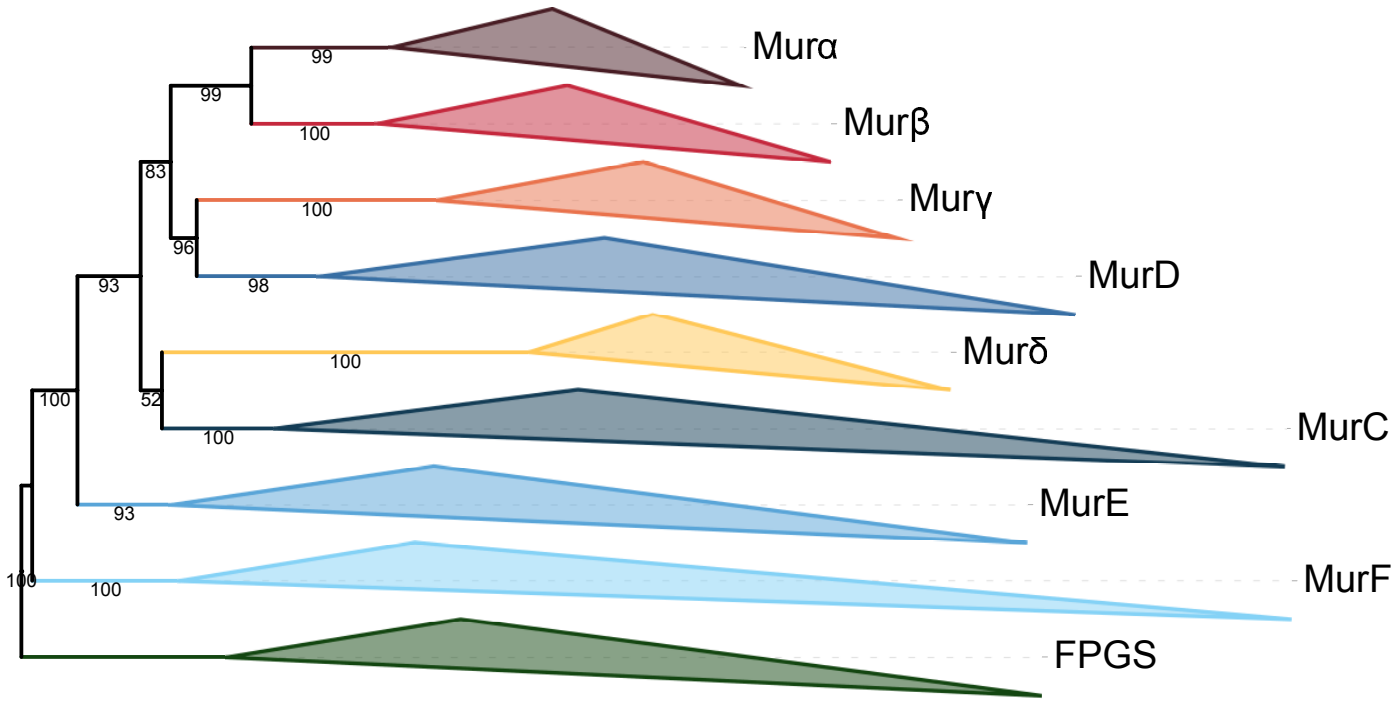

b

Tree scale: 1

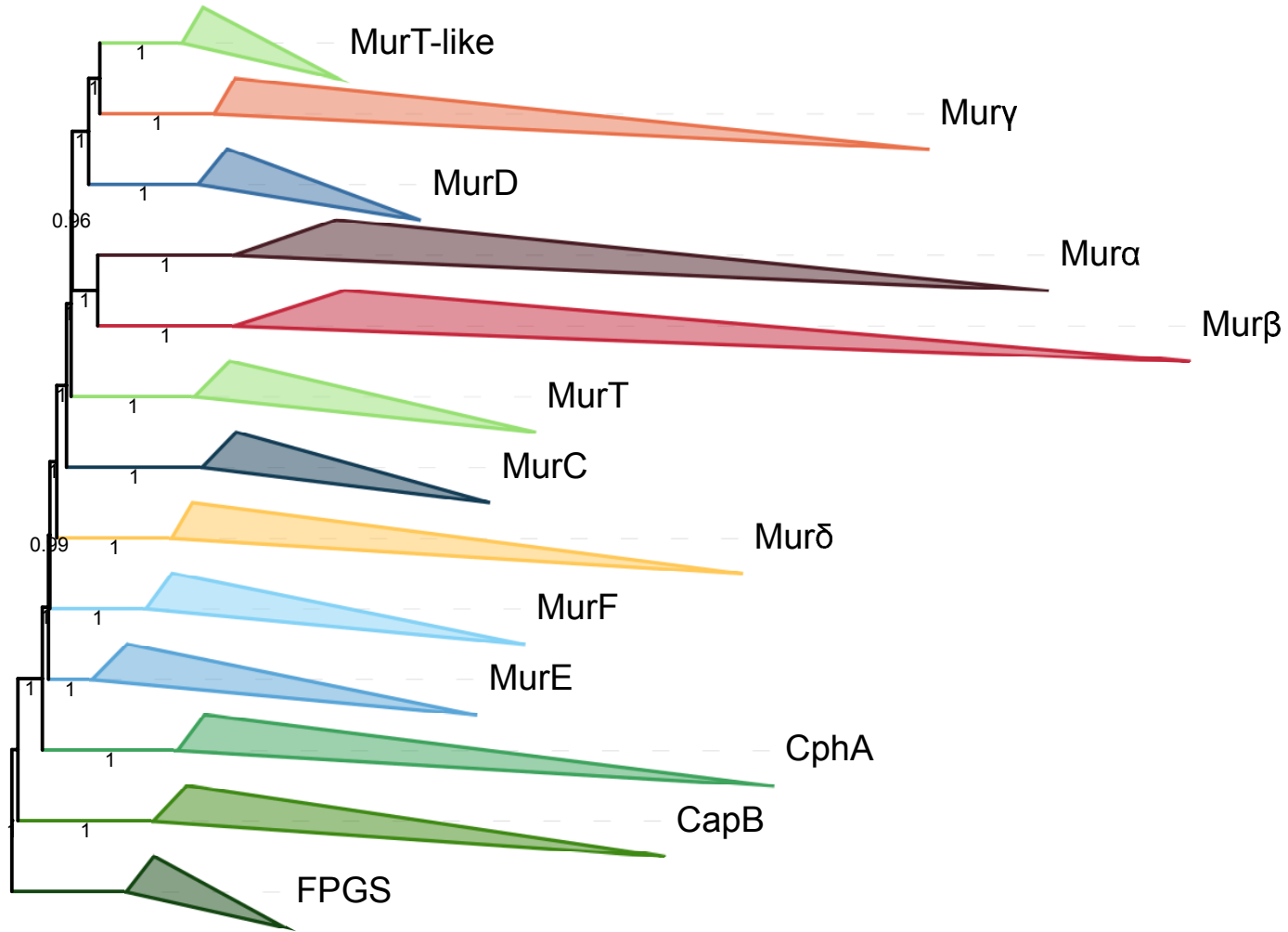

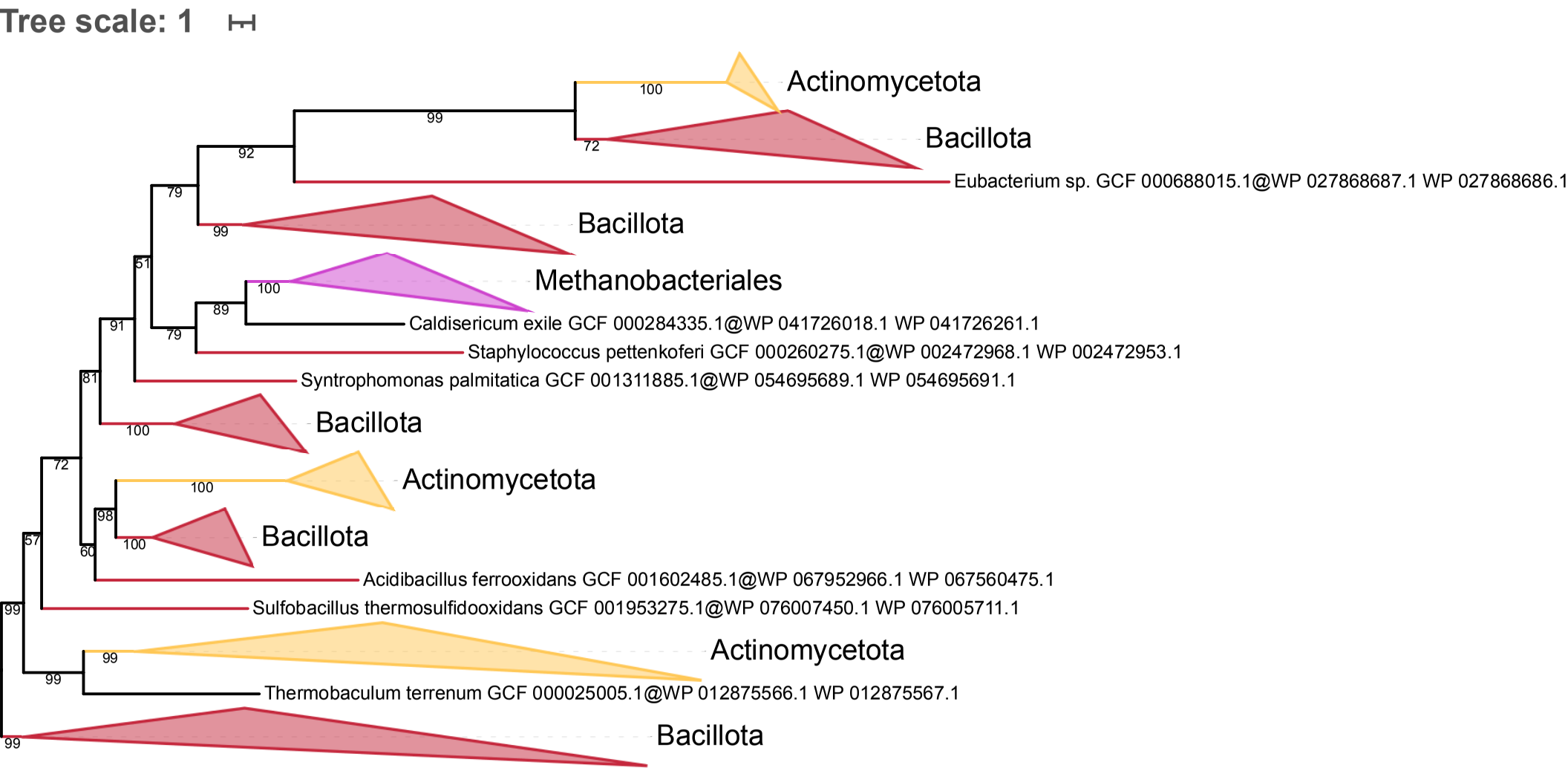
Tree scale: 1
Actinomycetota
Bacillota
Eubacterium sp. GCF 000688015.1@WP 027868687.1 WP 027868686.1
Bacillota
Methanobacteriales
Caldisericum exile GCF 000284335.1@WP 041726018.1 WP 041726261.1
Staphylococcus pettenkoferi GCF 000260275.1@WP 002472968.1 WP 002472953.1
Syntrophomonas palmitatica GCF 001311885.1@WP 054695689.1 WP 054695691.1
Bacillota
Actinomycetota
Bacillota
Acidibacillus ferrooxidans GCF 001602485.1@WP 067952966.1 WP 067560475.1
Sulfobacillus thermosulfidooxidans GCF 001953275.1@WP 076007450.1 WP 076005711.1
Actinomycetota
Thermobaculum terrenum GCF 000025005.1@WP 012875566.1 WP 012875567.1
Bacillota

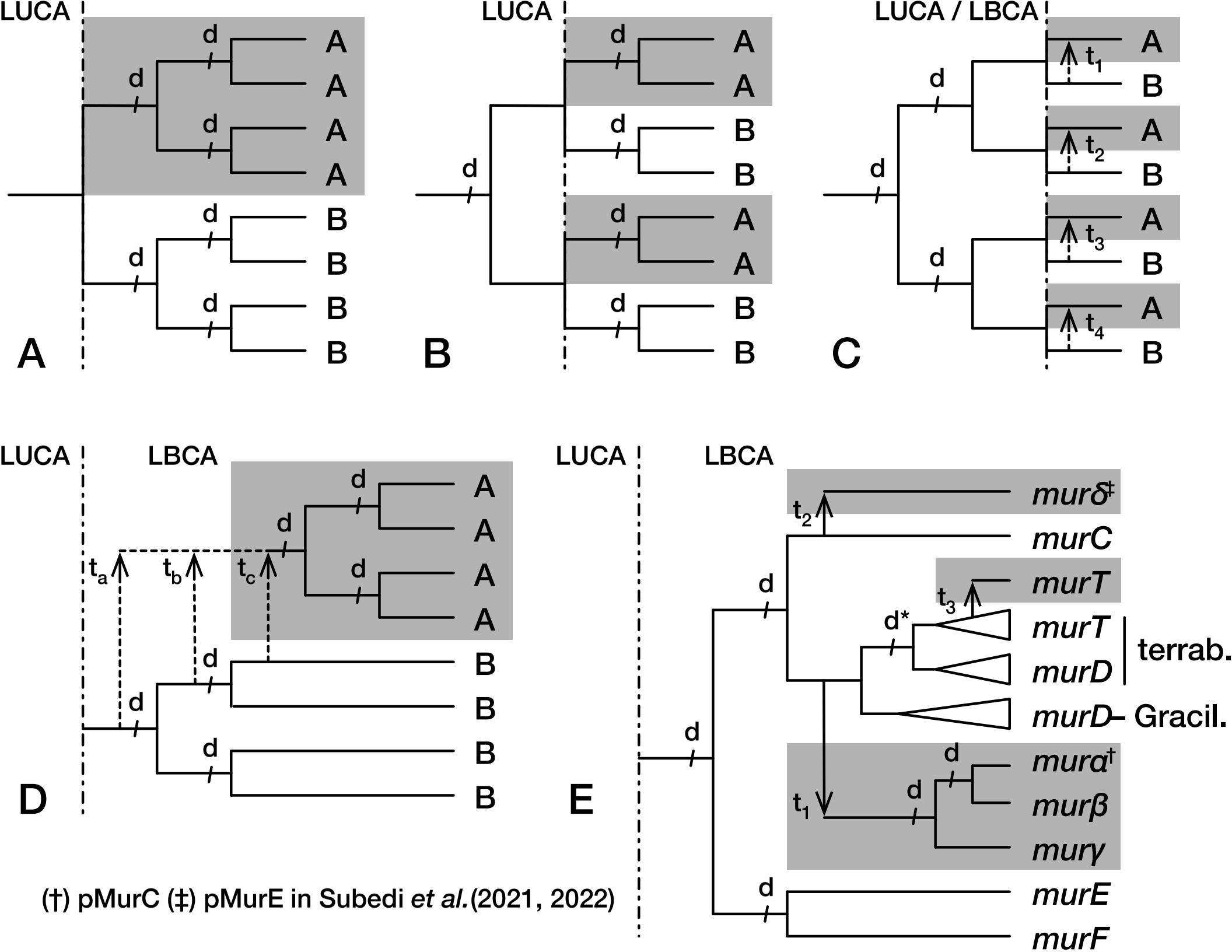

(†) pMurC (‡) pMurE in Subedi *et al.*(2021, 2022)